Anisotropic continuum damage constitutive model to describe the cyclic response of quasi-brittle materials: The regularized unilateral effect

Eliass Zafati, Benjamin Richard

Anisotropic continuum damage constitutive model to describe the cyclic response of quasi-brittle materials: the regularized unilateral effect

Eliass Zafati[a,b], Benjamin. Richard[c,*]

[a] *DEN-Service d'études mécaniques et thermiques (SEMT), CEA, Université Paris-Saclay, F-91191 Gif-sur-Yvette, France*
[b] *LMT-Cachan ENS Paris-Saclay/CNRS/PRES Université Paris Saclay 61, Avenue du Président Wilson, 94230 Cachan, France*
[c] *IRSN, 31 avenue du Général Leclerc, BP 17 F-92260, Fontenay aux Roses, France*

Abstract

Within the framework of damage mechanic, numerous anisotropic damage models have been proposed in the literature with the aim to represent the anisotropic degradation of quasi-brittle materials. The benefits from such models arise from the fact they are consistent with the principles of the continuum mechanics enabling easy numerical implementation in the majority of finite element codes. Despite the wealth of anisotropic models in the literature, further developments are needed to simulate correctly the responses involving phenomena related to crack closure. The present paper proposes a new class of anisotropic damage models characterized by its capabilities to describe non linear progressive stiffness recovery with the possibility to introduce permanent strains. The theoretical framework takes benefits from some results of the operator function theory. Further mathematical features are established for sets of functions, which are termed opening (closure) cracking functions. These features are useful to control the material behavior when the tensile or the compressive strains are activated (deactivated) with more or less smoothness. The thermodynamical admissibility condition is fulfilled, as long as the damage variable and the cracking functions satisfy further conditions. The robustness associated with the time integration of the proposed class of models is illustrated by a structural case study.

Keywords: Damage mechanics, anisotropic damage, operator function theory

*Corresponding author
Email address: benjamin.richard@irsn.fr (Benjamin. Richard)

Nomenclature

$\mathbb{R}^n$	Real space of n dimensions
$\mathcal{S}_n$	Space of second order symmetric tensors on the space $\mathbb{R}^n$
$\mathcal{S}_n^+$	Space of positive second order symmetric tensors on the space $\mathbb{R}^n$
$\boldsymbol{I}$	Identity second order tensor on $\mathbb{R}^n$
$\boldsymbol{\epsilon}$	Strain tensor
$\boldsymbol{\sigma}$	Stress tensor
$\boldsymbol{D}$	Second order damage tensor
$\boldsymbol{H}$	Second order integrity tensor
$\circ$	Schur product (Hadamard product)
$\mathrm{tr}\,(\cdot)$	Trace operator
$\|\cdot\|$	Bound norm
$\|\cdot\|_2$	Frobeinus norm
$\langle\cdot,\cdot\rangle$	Scalar product on $\mathbb{R}^n$
$\mathcal{C}^+$	Set of opening cracking functions
$\mathcal{C}^-$	Set of closure cracking functions
$\widetilde{D}_x$	The differential operator with respect to the variable x
E	Young's modulus
ρ	Mass density
ν	Poisson's ratio
η	Material parameter controlling the unilateral effect
$\hat{\epsilon}$	Mazars's equivalent strain
κ_0	Damage threshold
λ, μ	Lamé's coefficients
ψ	Free Helmohltz energy
s	Triaxiality exponent
S	Damage strength
T_X	Stress triaxiality

1. Introduction

Within the framework of structural design, efficient numerical analysis requires robust constitutive material models to predict satisfactorily the non linear behavior of structures under static or dynamic loading. In the case of quasi-brittle materials, the defects evolve and have preferential orientation due to mechanical boundary conditions and shrinkage effects. The evolution of these micro-defects results in stiffness degradation which itself leads to a non linear response of the structure [1]. When compressive loading is applied, the cracks close or partially close (if the permanent strains are considered), leading to the stiffness recovery. This phenomenon is known as the unilateral effect and has to be considered in the numerical computations when dealing with cyclic loads. Although many damage models, especially isotropic ones ([2, 3, 4, 5, 6, 7]), have been developed to reproduce the crack closure effect, further efforts still need be made to simulate correctly the structure response under cyclic loads. Besides this specific feature, additional ones can be summarized as follows:

1. stiffness degradation due to the development of the defects,
2. anisotropic behavior in the sense that the degradation depends on the directions,
3. dissymmetry between tension and compressive response,
4. permanent strains when unloading,
5. continuity of stress with respect to both strain and damage variables,
6. single damage variable to describe the damage process whatever the complexity of the loading path [8].
7. Regularized unilateral effect defined as a smooth crack opening/closing behavior (see also [6]).

The concept of continuum damage mechanics has been developed to describe the material degradation in an equivalent continuous media, by means of internal variables which deteriorate the material stiffness. This is generally achieved by using a scalar damage variable when a random distribution of micro-cracks is assumed or using a more or less complex variable (tensor) leading to a more realistic representation of the material anisotropy. As reported by several researchers, elasticity coupled with damage is generally sufficient to describe the concrete behavior, especially when the tension is the main cause of structural failure. During the last decades, several anisotropic models have been proposed in the literature. The anisotropy is generally introduced either by a fourth-order tensor [9, 10, 11, 12, 13] or a second-order damage tensor [8, 14, 15, 16, 17, 18, 19, 20, 21, 22].

However, the second-order formulations still remains the most popular due to its simplicity to represent three orthogonal families of microcracks and its capabilities to model in a realistic way the behavior of metals or quasi-brittle materials. One of the earliest development concerns the extension of the concept of equivalence between fictitious undamaged configuration and the real damaged configuration in three dimensions suggested by Murakami [15] leading to the definition of an effective stress tensor using a symmetric second order damage tensor. Based upon the effective stress concept, Lemaitre *et al.* [17] proposed one of the most popular damage-based anisotropic model for metallic materials established within the framework of the strain equivalence principle, where the elasticity is written through a partition technique between the deviatoric part and the hydrostatic part of the elastic energy. However, the relations controlling the damage evolution does not prevent the damage variables from evolving beyond the unity and losing their physical meaning. Consequently, additional improvements have been proposed recently by Desmorat [8] where the damage state is described using the integrity tensor instead of the damage tensor. An attempt to couple the hysteretic effects (due to frictional mechanisms between the lips of the cracks) with anisotropic damage has been suggested by Halm *et al.* [19], using a spectral decomposition. Nonetheless, some thermodynamical inconsistencies reflected by the non uniqueness of the potential have been reported by Cormery *et al.* [23]. Similar drawbacks were expressed regarding the anisotropic model developed by Chaboche [24]. In order to move forward, enhancements of the original Halm's model have been proposed by Bargellini *et al.* [18] using fixed micro-crack directions in such a way that the damage evolution is controlled by functions, called micro-crack densities. Although the majority of existing anisotropic damage models focus on the description of the anisotropic character of quasi-brittle materials, many formulations which take into account the unilateral effect may be found in the literature [10, 25, 26, 20]. For the majority of the anisotropic model, the unilateral effect is mainly introduced by a decomposition technique (or projection technique) into positive and negative part of the strain or the stress tensor. As observed by Chaboche [10], some models have been developed using the latter technique suffer from some inconsistency regarding the symmetry of the secant stiffness. Moreover, the use of the projection technique results in a discontinuous secant stiffness leading to an abrupt crack closure and some difficulties of convergence as observed by Jefferson and Mihai [6].

In order to ensure the boundedness of the damage tensor (generally bounded by unity in norm) and to keep a physical meaning of the results, different strategies can be founded in the literature. One of the easiest options is to control the rate of the integrity tensor

$\boldsymbol{H} = (\boldsymbol{I} - \boldsymbol{D})^{-\frac{1}{2}}$ or the pseudo-logarithmic damage tensor instead of the damage tensor $\boldsymbol{D}$ (see [27, 28, 8]). An other strategy using the characteristic function has been suggested by Badel *et al.* [20]. In general, the damage evolution is controlled by an associated tensor which can be expressed in the form $\phi = (\boldsymbol{I} - \boldsymbol{D})^p$, where p is a real (see also [16, 29, 30, 31]). It is seen that the rate $\dot{\phi}$ depends on the exponent p and, in many cases, there is no equivalence between the positivity of $\dot{\phi}$ and $\dot{\boldsymbol{D}}$, i.e. for instance if $p = -\frac{1}{2}$ the positivity of $\dot{\phi}$ does not imply the positivity of $\dot{\boldsymbol{D}}$. This issue is also discussed farther in the paper.

Despite the wealth of the proposed second order damage formulations, in our knowledge none takes into account simultaneously a progressive smooth crack opening/closing behavior (the regularized unilateral effect) and the irreversible strains. In this regard, the paper aims to present a family of second order anisotropic damage models for quasi-brittle materials which satisfy the properties (1) to (7) described above. In the following, the paper is organized into three parts. The first part reviews some notions and basic results related to the operator and trace function theories. The second part is devoted to the construction of a new class of damage models characterized by its abilities to take into account the unilateral effect with the possibility to introduce permanent strains. Further fundamentals mathematical results concerning the well-posedness of the boundary problem at fixed damage state as well as the thermodynamical consistency in the sense of distributions are shown. The relation between the rates associated with the damage tensor and different form of the integrity tensor is also investigated. The last part is focused on the numerical examples to highlight the robustness of the model regarding smoothing of the crack opening-closing behavior and introducing permanent strains.

2. Operator and trace functions: definitions and basic results

The space $\mathcal{S}_n$ can be endowed with a partial order on $\mathcal{S}_n$ as follows: the tensor $A \in \mathcal{S}_n$ is said to be positive semi-definite if:

$$\langle x, Ax \rangle \geq 0 \qquad \forall\, x \in \mathbb{R}^n \tag{1}$$

and we write $A \geq 0$. A is said positive definite if the inequality (1) is strict for all $x \neq 0$ in $\mathbb{R}^n$ and we write $A > 0$. Finally, the space $\mathcal{S}_n$ is partially ordered by defining $A \geq B$ as $A - B \geq 0$.

Two tensors A and B from $\mathcal{S}_n$ are equivalent if there exists a non-singular tensor $R \in \mathcal{S}_n$, not necessary symmetric, such that:

$$A = R^T B R \tag{2}$$

As a consequence of the equation (2), if the tensor B is positive (resp. negative) then A is also positive (resp. negative), and conversely.

Let f be a real function on an interval J. If $A \in \mathcal{S}_n$, with its eigenvalues, denoted $\alpha_1, ..., \alpha_n$, are in J, we define the operator function f in $\mathcal{S}_n$ by:

$$f(A) = \sum_{i=1}^{n} f(\alpha_i)\, P_i \tag{3}$$

where P_i are the spectral projections of A. For any orthonormal basis, says $\{e_1, ..., e_n\}$, the trace function, defined on $\mathcal{S}_n$, and associated with the function f is given by:

$$tr(f(A)) = \sum_{i=1}^{n} \langle e_i, f(A) e_i \rangle \tag{4}$$

f is said to be a monotone operator function if for any tensors A and B such that $A \geq B$, we have $f(A) \geq f(B)$.

Let $J = (a, b)$ be an interval and f a continuously differentiable function on J. If $A \in \mathcal{S}_n$, with its eigenvalues, denoted $\alpha_1, ..., \alpha_n$, are in J, then the trace function defined above is also continuously differentiable whose differential is given by:

$$\widetilde{D}_A\, tr(f(A))(\tilde{H}) = tr\left(f^{'}(A)\tilde{H}\right) \tag{5}$$

Generally, if L^* is the adjoint of a linear operator L defined on $\mathcal{S}_n$ then:

$$\widetilde{D}_A\, tr(f(L(A))) = L^*(f^{'}(L(A))) \tag{6}$$

As an example which will be used later, let $L(A) = KAK$ for any symmetric tensor $K \in \mathcal{S}_n$, then L is symmteric and $L = L^*$.

Remark The relation between the convexity of f and $tr(f(.))$ is the most interesting feature of this class of functions. An immediate corollary of the Peierls's Inequality [32] shows that if f is convex (resp. strictly convex) then $A \to tr(f(A))$ is convex (resp. strictly convex). Furthermore if the map is assumed convex, a practical inequality implying the Peierls Inequality states that for any unitary vector u:

$$f\left(\langle u, Au \rangle\right) \leq \langle u, f\left(A\right) u \rangle \tag{7}$$

where the eigenvalues of A belong to the domain of f.

3. A new class of damage models and fundamental results

3.1. Motivations and definition of cracking functions

The unilateral effect is considered as an intrinsic feature of quasi-brittle materials such concrete. This phenomenon is described by the majority of isotropic (or anisotropic) damage models using a split technique between the compressive and the tension behaviors by means of the positive part function $x \longmapsto \langle x \rangle^+ = \max(x, 0)$. This function is generally introduced into the stress or strain tensor in order to distinguish the compressive strain (stress) from the tension strain (stress). Nonetheless, the lack of differentiability at $x = 0$ may cause numerical issues when (the secant) stiffness matrix is updated. Indeed, when the positive part function is applied to a tensor A, in the sense of the definition (3), it is seen that the resulting tensor, denoted $\langle A \rangle^+$, is positive and belongs to $\mathcal{S}_n^+$. It may be checked that $A \longmapsto \langle A \rangle^+$ is differentiable if and only if A is non singular. Thus, the stiffness operator is only meaningful for this set of tensors. Moreover, some references [33, 6] have discussed, from a numerical point of view, the benefits of smoothing the behavior of crack closure against an abrupt crack closure.

Given the aforementioned shortcomings, the aim of the following parts is to introduce new families of functions, called opening cracking functions (resp. closure cracking functions) playing a similar role as the function $x \longmapsto \langle x \rangle^+$ (resp. $x \longmapsto \langle x \rangle^- = \min(x, 0)$) enjoying more valuable features in term of smoothness as detailed later.

3.1.1. Opening cracking functions

Definition Let $\mathcal{C}^+$ be the set of the opening cracking real-valued functions f defined on $\mathbb{R}$, i.e., $\mathrm{dom}(f) = \mathbb{R}$, and satisfying the following properties:

1. f is convex on $\mathbb{R}$,
2. $\lim\limits_{x \to +\infty} (f(x) - x)$ is finite,
3. f is integrable in the neighborhood of $-\infty$.

$\mathcal{C}^+$ is clearly convex and not empty since the function $f(x) = \max(x, 0)$ fulfills all the aforementioned items. It will be shown that, in addition to the statements (1), (2) and (3), valuable features characterizing the opening cracking functions can be derived which provide new information on the regularity of such functions or their behaviors at $-\infty$. Recall that the interest of such functions is to build, not a single, but a class of elastic damage models that fit into the thermodynamic framework and satisfy some classical properties such as the positivity of the potential energy and the convexity with respect to the strain tensor. Since no regularity is imposed, each model from the previous class may

differ from each other in terms of capabilities of smoothing the responses when switching from tension to compression. Further properties of the opening cracking functions are given in the following proposition.

Proposition 3.1. *Let f be of $\mathcal{C}^+$, then:*

1. *f belongs to $C^0(\mathbb{R})$, i.e., f is continuous on $\mathbb{R}$,*
2. *f is a non decreasing positive function and $\lim_{x\to-\infty} f(x) = 0$,*
3. *$F(x) = \int_{-\infty}^{x} f(u)\,du$ is a convex positive function,*
4. *f is a 1-Lipschitz function.*

Proof :

1. The continuity results from the convexity of f [34].
2. Let $(x_n)_n$ be a strictly non increasing sequence such that $\lim_{n\to+\infty} x_n = -\infty$. If there exists an integer $p \geq 1$ such as $f(x_{p+1}) \geq f(x_p)$, then $(f(x_n))_{n\geq p}$ is non decreasing sequence. Indeed, since $x_{p+2} < x_{p+1} < x_p$, there exists $t \in]0,1[$ such $x_{p+1} = t\,x_p + (1-t)\,x_{p+2}$. Thus, using the convexity of f, we conclude that $(f(x_{p+2}) - f(x_{p+1})) \geq \frac{t}{(1-t)}\,(f(x_{p+1}) - f(x_p)) \geq 0$. By induction, the result remains valid for all $n \geq p$.
   In all cases, it is seen that $(f(x_n))_n$ admits a limit $l \in \overline{\mathbb{R}}$ which is not necessary finite when n goes to $+\infty$. The next step consists in establishing that two sequences $(p_n)_n$ and $(q_n)_n$ of the same nature as $(x_n)_n$ have the same limit. For this purpose, we build another sequence $(z_n)_n$ of the same nature as $(x_n)_n$ such that $(z_{2n})_n$ and $(z_{2n+1})_n$ are sub-sequences of $(p_n)_n$ and $(q_n)_n$, respectively (this is possible by construction). It is clear that $(z_n)_n$ has at least two adherent points in $\overline{\mathbb{R}}$ which are the limits of $(p_n)_n$ and $(q_n)_n$. Moreover, $(z_n)_n$ converges (since $(z_n)_n$ shares the same properties of $(x_n)_n$) with a unique adherent point. Thus, both sequences $(p_n)_n$ and $(q_n)_n$ have the same limit l as $(x_n)_n$ which is evidently the limit of f when $x \to -\infty$ since f is continuous. Moreover, if $l \neq 0$ then the function f cannot be integrable in the neighborhood of $-\infty$ which contradicts the definition of $\mathcal{C}^+$. Hence, for all $(x,y) \in \mathbb{R}^2$ we have:

$$\frac{f(x) - f(y)}{x - y} \geq \lim_{z\to-\infty} \frac{f(z) - f(y)}{z - y} = 0 \tag{8}$$

   In the equation (8), we use the fact that the map $x \longmapsto \frac{f(x)-f(y)}{x-y}$ increases with x (classical result from the convex function theory). Given this result, we deduce that f is a non decreasing positive function since $f(x) \geq f(-\infty) = 0$.

3. Since f is positive, then $F(x) = \int_{-\infty}^{x} f(u)\,du \geq 0$. Moreover, the monotony of f, previously demonstrated, implies the convexity of F.
4. Using the assumption $\lim\limits_{x\to+\infty} (f(x) - x) < +\infty$, we infer:

$$1 = \lim_{z\to+\infty} \frac{f(z) - f(y)}{z - y} \geq \frac{f(x) - f(y)}{x - y} \geq 0 \tag{9}$$

Thus,

$$|f(x) - f(y)| \leq |x - y| \tag{10}$$

□

Before going further, same comments on the physical interpretation of the previous proposition can be given. Since the present model is built using the Helmohltz free energy (expressed in term of the strain tensor), the continuity of the opening cracking functions is needed to ensure the continuity of the stress tensor with respect to the strain tensor, as highlighted later. The second property shows, in conjunction with the role played by the positive part function, that any function from this family is deactivated once the compressive strains become sufficiently large. The third property is useful to build a positive convex free energy with respect to the strain tensor using the primitives of the form $F(x) = \int_{-\infty}^{x} f(u)\,du$. Finally, the assertion 4 implies that f is differentiable almost everywhere in the sense of Lebesgue measure. This is also a direct consequence of a deeper result in the convex analysis (see [34]). For practical applications, we restrict ourselves to smooth functions that belong, at least, to the space $C^1(\mathbb{R})$ except for a finite set of points.

From a physical point of view, the second assumption of the above definition indicates that the term $f(x)$ is approximately equal to x up to a constant when the tension strains are sufficiently significant. This condition, when considered without further assumptions, is not sufficient to conclude that $f'(x)$ is close to 1 when x is sufficiently large and thus to provide information on the behavior of the secant stiffness for a fixed damage state. In order to achieve a better convergence of the Hessian operator, it is necessary to control the behavior of the derivative at $(\pm\infty)$ in order to satisfy similar properties as the ones fulfilled in case of the positive part function. In this case, the derivative of each function should converge to unity for important tension strains and vanish (or converge to 0) for compressive strains. This is ensured by the following proposition:

Proposition 3.2. *Let f be an element of $\mathcal{C}^+$, which is differentiable except in finite number of points, then:*

$$\lim_{x\to+\infty} f^{'}(x) = 1 \tag{11a}$$

$$\lim_{x\to-\infty} f^{'}(x) = 0 \tag{11b}$$

Proof :

We restrict ourselves to the first assertion since the second holds by analogy. For $n \in \mathbb{N}$ sufficiently large, using the mean value theorem, there exists an increasing sequence $(\xi_n)_n$ such that $n < \xi_n < n+1$ and:

$$\frac{f(n+1) - f(n)}{n+1-n} = f^{'}(\xi_n) \tag{12}$$

Taking into account the fact that f is convex, $f^{'}$ is an increasing function, which means that $\lim_{x\to+\infty} f^{'}(x)$ exits and equals to $\lim_{n\to+\infty} f^{'}(\xi_n)$.

In other hand, we have:

$$f(n) - n = c + \circ(1) \tag{13}$$

for some constant c. Thus, using the above relation for n and $n+1$, respectively, we deduce $f^{'}(\xi_n) = \frac{f(n+1)-f(n)}{n+1-n} = 1 + \circ(1)$. □

Remark :

Because $f^{'}$ increases with x and $f^{'}(-\infty) = 0$, the derivative $f^{'}$ is non-negative which means that the function F is convex (since $F^{''} = f^{'}$) as claimed by the proposition 3.1. Moreover, it should be noted that the relations (11a) and (11b) do not always hold without the convexity assumption. □

3.1.2. Closure cracking functions

In the same spirit, we define $\mathcal{C}^-$, the set of the closure cracking functions f satisfying the following properties:

- f is concave on $\mathbb{R}$,
- $\lim_{x\to-\infty} f(x) - x$ is finite,
- f is integrable in the neighborhood of $+\infty$.

From the definition above, the set $\mathcal{C}^-$ is also convex characterized by the following properties:

Proposition 3.3. *Let f be of $\mathcal{C}^-$, then:*

1. *f belongs to $C^0(\mathbb{R})$, i.e., f is continuous on $\mathbb{R}$,*
2. *f is a non decreasing negative function and $\lim_{x\to+\infty} f(x) = 0$,*
3. *$F(x) = \int_{+\infty}^{x} f(u)\,du$ is a convex positive function,*
4. *f is a 1-Lipschitz function.*

Proof : similar to proposition 3.1 □

Furthermore, if each function $f \in \mathcal{C}^-$ belongs to $C^1(\mathbb{R})$ except in a finite set of points, then:

Proposition 3.4. *Let f be an element of $\mathcal{C}^-$, which verifies the above assumption, then:*

$$\lim_{x\to+\infty} f'(x) = 0 \tag{14a}$$

$$\lim_{x\to-\infty} f'(x) = 1 \tag{14b}$$

Proof : similar to proposition 3.2 □

3.2. The free energy expression

One of the challenges encountered in the thermodynamical formulation for quasi-brittle material models is the description of the unilateral effect using single damage variable [35]. In this section, the free energy associated with the new class of damage models is elaborated by means of the cracking functions, introduced in section 3.1. The unilateral effect is taken into account by splitting the free energy, denoted $\psi(\boldsymbol{\epsilon}, \boldsymbol{H})$, into two different parts. The first part affected by the second order integrity tensor H, related to the damage tensor $\boldsymbol{D}$ and defined by $\boldsymbol{H} = (\boldsymbol{I} - \boldsymbol{D})^{-\frac{1}{2}}$ as pointed out in the introduction, describes the behavior of the material as long as the tension strains are activated. The second part, partially affected by the second order damage tensor, describes the behavior when compressive strains are activated. Theoretical results from the previous section are used to describe the main properties of the free energy, regarding to the smoothness and the convexity character. Further mathematical results concerning the boundary value problem are also investigated.

Let $\boldsymbol{\epsilon}$ be the strain tensor and $\boldsymbol{H}$ the integrity tensor, the free energy potential $\psi(\boldsymbol{\epsilon}, \boldsymbol{H})$ is defined by:

$$\psi(\boldsymbol{\epsilon}, \boldsymbol{H}) = \psi^{+}_{F^+,G^+}(\boldsymbol{\epsilon}, \boldsymbol{H}) + \psi^{-}_{F^-,G^-}(\boldsymbol{\epsilon}) \tag{15}$$

where,

$$\rho\psi^{+}_{F^{+},G^{+}}\left(\boldsymbol{\epsilon},\boldsymbol{H}\right)=2\mu\, tr\left(F^{+}\left(\boldsymbol{H}^{-\frac{1}{2}}\boldsymbol{\epsilon}\boldsymbol{H}^{-\frac{1}{2}}\right)\right)+\lambda\,\frac{3}{tr\left(\boldsymbol{H}^{2}\right)}\,G^{+}\left(tr\left(\boldsymbol{\epsilon}\right)\right) \tag{16}$$

and,

$$\rho\psi^{-}_{F^{-},G^{-}}\left(\boldsymbol{\epsilon},\boldsymbol{H}\right)=2\mu\,\left(1-\eta\left\|\boldsymbol{D}\right\|\right)\,tr\left(F^{-}\left(\boldsymbol{\epsilon}\right)\right)+\lambda\,G^{-}\left(tr\left(\boldsymbol{\epsilon}\right)\right) \tag{17}$$

where $F^{+}:x\longmapsto\int_{-\infty}^{x}f^{+}\left(u\right)du$ and $G^{+}:x\longmapsto\int_{-\infty}^{x}g^{+}\left(u\right)du$, where f^{+} and g^{+} are the opening cracking functions selected from the set $\mathcal{C}^{+}$, while $F^{-}:x\longmapsto\int_{+\infty}^{x}f^{-}\left(u\right)du$ and $G^{-}:x\longmapsto\int_{+\infty}^{x}g^{-}\left(u\right)du$ where f^{-} and g^{-} are the closure cracking functions selected from the set $\mathcal{C}^{-}$. The functions F^{+} and F^{-} are viewed as operator functions (see definitions (3) and (4)). The parameters λ and μ are the Lamé coefficients for undamaged material and η is a positive parameter selected between 0 and 1. As mentioned above, the potential $\psi^{+}_{F^{+},G^{+}}\left(\boldsymbol{\epsilon},\boldsymbol{H}\right)$ represents the behavior affected by the damage controlled by the tensor $\boldsymbol{H}$, while $\psi^{-}_{F^{-},G^{-}}\left(\boldsymbol{\epsilon}\right)$ represents the behavior partially affected by the damage. As will be highlighted later in the numerical examples, the parameter η has been introduced to control the degree of the unilateral effect which is total when $\eta=1$ and partial when $\eta<1$. Note that the non linearity of the cracking functions has the advantage to reproduce a progressive crack opening that match the experimental observations [36]. Moreover, smoothing the behavior has also the benefit to improve the numerical convergence comparing with the damage models with abrupt contact as reported by [6]. This can be achieved by selecting sufficiently smooth cracking functions, at least of class C^{1}, to ensure the continuous differentiability of the functional $\psi\left(\boldsymbol{\epsilon},\boldsymbol{H}\right)$ in one hand and the continuity of the corresponding Hessian tensor on the other hand.

Note that the tensor $\boldsymbol{H}^{-\frac{1}{2}}\boldsymbol{\epsilon}\boldsymbol{H}^{-\frac{1}{2}}$ in the relation (16) is equivalent to the strain tensor $\boldsymbol{\epsilon}$ following the definition given in section 2. Thus, it is clear that if the tensor $\boldsymbol{\epsilon}$ is negative semi-definite (i.e. $-\boldsymbol{\epsilon}$ est positive semi-definite), the stress tensor related to the damaged part tends to vanish when the eigenvalues of $\boldsymbol{\epsilon}$ are negatives and sufficiently high. Conversely, if $\boldsymbol{\epsilon}$ is positive, the stress tensor related to the undamaged (or partially damaged) part becomes inactive when the eigenvalues of $\boldsymbol{\epsilon}$ are positive and sufficiently large.

Remark : The concept of *special positive part* of the stress tensor, denoted σ^{+}, has been proposed by Ladevèse [16] which is built using the positive part of eigenvalues of the tensor $\boldsymbol{H\sigma}$. Indeed, it can be verified that the previous definition is related to the positive part function (see Appendix A) by:

$$tr\left(\boldsymbol{H}_1\boldsymbol{\sigma}^+\boldsymbol{H}_1\boldsymbol{\sigma}^+\right) = tr\left(\left(\left\langle \boldsymbol{H}_1^{\frac{1}{2}}\boldsymbol{\sigma}\boldsymbol{H}_1^{\frac{1}{2}}\right\rangle^+\right)^2\right) \tag{18}$$

□

One can notice that the proposed Helmholtz free energy ψ has the property to be independent on the basis in which it is expressed. In other words, one can observe that $\psi\left(\boldsymbol{\epsilon},\boldsymbol{H}\right) = \psi\left(\boldsymbol{U}^T\boldsymbol{\epsilon}\,\boldsymbol{U},\boldsymbol{U}^T\boldsymbol{H}\,\boldsymbol{U}\right)$ for all orthogonal tensor $\boldsymbol{U}$ in the special orthogonal group. The convexity with respect to the strain tensor is ensured for all of cracking functions (see the remark in section 2), while the strict convexity can be ensured if one the functions F^+ or F^- is strictly convex. It is worth noticing that the strict convexity of the potential is generally essential (of course with further assumptions) to construct a one to one and onto operator between the strain and the stress tensor spaces. Due to thermodynamic requirement (see section 3.3), the function F^+ can only be strictly convex in $\mathbb{R}^+$. This constraint, combined with a weak assumption on F^-, provides a strict convexity of the potential as stated by the proposition 3.5.

Proposition 3.5. *If f^+ and f^- are strictly monotone on $\mathbb{R}^+$ and $\mathbb{R}^-$, respectively; then the potential ψ is strictly convex on $\mathcal{S}_n$ for a fixed $\boldsymbol{H}$.*

Proof : see Appendix B

The stress tensor can be derived using the expression of the free energy (15). Here, we assume that the stress tensor is related to the damage tensor $\boldsymbol{H}$ and the strain tensor $\boldsymbol{\epsilon}$ by:

$$\begin{aligned}\boldsymbol{\sigma}(\boldsymbol{\epsilon},\boldsymbol{H}) &= \widetilde{D}_{\boldsymbol{\epsilon}}\psi(\boldsymbol{\epsilon},\boldsymbol{H}) \\ &= 2\mu\,\boldsymbol{H}^{-\frac{1}{2}} f^+\left(\boldsymbol{H}^{-\frac{1}{2}}\boldsymbol{\epsilon}\boldsymbol{H}^{-\frac{1}{2}}\right)\boldsymbol{H}^{-\frac{1}{2}} + \lambda\,\frac{3}{tr\left(\boldsymbol{H}^2\right)}\,g^+\left(tr\left(\boldsymbol{\epsilon}\right)\right)\,\boldsymbol{I} \\ &\quad +2\mu\,\left(1-\eta\,\|\boldsymbol{D}\|\right)\,f^-\left(\boldsymbol{\epsilon}\right) + \lambda\,g^-\left(tr\left(\boldsymbol{\epsilon}\right)\right)\,\boldsymbol{I}\end{aligned} \tag{19}$$

The first term is obtained using the equation (6) with the linear operator $L(\boldsymbol{\epsilon}) = \boldsymbol{H}^{-\frac{1}{2}}\boldsymbol{\epsilon}\boldsymbol{H}^{-\frac{1}{2}}$ whereas the other terms are derived straightforwardly using the equation (5). It should be noticed that the stress tensor is continuous with respect to the damage and strain tensors, since the cracking functions and the norm $\|.\|$ are continuous. The proposition 3.6 shows that the stress tensor, when considered as an operator, is Liptchiz with respect to the strain tensor.

Proposition 3.6. *We claim:*

- *Each function* $f \in \mathcal{C}^+ \cup \mathcal{C}^-$ *satisfies* $\|f(A) - f(B)\|_2 \leq \|A - B\|_2$ *for any couple* $(A, B) \in (\mathcal{S}_n)^2$.

- *The operator* $\widetilde{D}_{\boldsymbol{\epsilon}}\psi(., \boldsymbol{H})$ *is Lipschitz with respect to* $\boldsymbol{\epsilon}$ *and we have, for some constant* $C(\boldsymbol{H}, \lambda, \mu)$ *that is continuous with respect to* $\boldsymbol{H}$ *for every* λ *and* μ*:*

$$\left\|\widetilde{D}_{\boldsymbol{\epsilon}}\psi(\boldsymbol{\epsilon}_2, \boldsymbol{H}) - \widetilde{D}_{\boldsymbol{\epsilon}}\psi(\boldsymbol{\epsilon}_1, \boldsymbol{H})\right\|_2 \leq C \|\boldsymbol{\epsilon}_2 - \boldsymbol{\epsilon}_1\|_2$$

for all $(\boldsymbol{\epsilon}_1, \boldsymbol{\epsilon}_2) \in (\mathcal{S}_n)^2$.

Proof :

The proof of the first assertion focus on the set $\mathcal{C}^+$ (similar proof is applied to $\mathcal{C}^-$) and can be achieved in two steps:

Step 1: The set $\mathcal{C}^+ \cap C^\infty(\mathbb{R})$ is dense in $\mathcal{C}^+$ with respect to the uniform norm.

Let $f \in \mathcal{C}^+$ and $\rho_c \in C^\infty(\mathbb{R})$ a positive function such $supp(\rho_c) \subset (-1, 1)$ and $\int_{\mathbb{R}} \rho_c dx = 1$. We introduce a sequence of infinitely differentiable functions $(f_n)_n$ defined on $\mathbb{R}$ by: $f_n(x) = \int_{\mathbb{R}} \rho_c(n(x-y)) f(y) dy$

We claim that f_n belongs to $\mathcal{C}^+ \cap C^\infty(\mathbb{R})$ for each n. Indeed, we have $f_n(x) = \int_{\mathbb{R}} \rho_c(ny) f(x-y) dy$. Using the definition of the convexity and the positivity of ρ_c, it is clear that f_n is convex. Since $x \longmapsto f_n(x) - x$ is convex, the limit $\lim_{x \to +\infty} (f_n(x) - x)$ exists. In addition, we have $f_n(x) - x = \int_{\mathbb{R}} \rho_c(n(x-y))(f(y) - f(x))dy + f(x) - x$. It is seen that the last term is bounded due to the definition of f and the first is also bounded by $\left|\int_{\mathbb{R}} \rho_c(n(x-y))(f(y) - f(x))dy\right| \leq \int_{\mathbb{R}} \rho_c(n(x-y))|x-y| dy \leq \frac{1}{n}$. Thus the limit $\lim_{x \to +\infty} (f_n(x) - x)$ is finite. The integrability of f_n in the neighborhood of $-\infty$ is a direct consequence of the Fubini's theorem.

To conclude we have:

$$|f_n(x) - f(x)| = \left|\int_{\mathbb{R}} \rho_c(n(x-y))(f(y) - f(x))dy\right| \leq \frac{1}{n} \tag{20}$$

which leads to $\lim_{n \to +\infty} |f_n - f|_\infty = 0$.

Step 2: Let $f \in \mathcal{C}^+$ and $(f_n)_n$ be the sequence defined in *step* 1 which converges uniformly to f. For each couple $(A, B) \in (\mathcal{S}_n)^2$ we have:

$$f_n(B) - f_n(A) = \int_0^1 \widetilde{D} f_n(B + t(B - A))(B - A) dt \tag{21}$$

Using theorem in [37], it is easy to check that:

$$\|f_n(A) - f_n(B)\|_2 \leq \sup_{t \in \mathbb{R}} \left|f_n'(t)\right| \|A - B\|_2 \tag{22}$$

Taking into account the property 4 in proposition 3.1 we deduce $\sup_{t\in\mathbb{R}}\left|f_n^{'}(t)\right|\leq 1$. Taking the limit to infinity, we obtain the result.

The proof of the second assertion is a consequence of the previous one. Indeed, each function from $\mathcal{C}^+\cup\mathcal{C}^-$ is 1-Lipschitz. As a consequence, there exists a constant C with the desired features such as for all couple $(\boldsymbol{\epsilon}_1,\boldsymbol{\epsilon}_2)\in(\mathcal{S}_n)^2$, we have:

$$\left\|\widetilde{D}_{\boldsymbol{\epsilon}}\psi(\boldsymbol{\epsilon}_2,\boldsymbol{H})-\widetilde{D}_{\boldsymbol{\epsilon}}\psi(\boldsymbol{\epsilon}_1,\boldsymbol{H})\right\|_2\leq C(\boldsymbol{H})\left\|\boldsymbol{\epsilon}_2-\boldsymbol{\epsilon}_1\right\|_2 \tag{23}$$

□

For small strains, the strain tensor $\boldsymbol{\epsilon}$ is the linear operator defined on a displacement field vector u, such as $\boldsymbol{\epsilon}(\boldsymbol{u})=\frac{1}{2}\left(\nabla\boldsymbol{u}+\nabla^T\boldsymbol{u}\right)$. Let P_{rigid} be the vector space defined by $P_{rigid}=\left\{\boldsymbol{u}\in\left(W^{1,2}(\Omega)\right)^n/\boldsymbol{u}(x)=a+b\times x\right\}$ which represents the rigid-body motions. Let Ω be bounded and open domain characterized by a Lipschitz boundary Γ divided into disjoint parts Γ_u, Γ_τ and $\mathcal{T}$. Γ_u, Γ_τ are open while $\mathcal{T}$ has a measure equal to zero. Let W and P be the vector spaces defined by $W=\left\{\boldsymbol{u}\in\left(W^{1,2}(\Omega)\right)^n/\boldsymbol{u}\mid_{\Gamma_u}=0\right\}$ and $P=W\cap P_{rigid}$. P is a finite dimensional space and consequently, admits and orthogonal complement $P^\perp$ in W. Assuming that $\boldsymbol{H}$ is an element of the space $V_{\boldsymbol{H}}=\{X\in L^\infty(\Omega,\mathcal{S}_n)/\ X\geq I\}$.

Now, we consider the following problem (P^*). Find $u\in\left(W^{1,2}(\Omega)\right)^n$ such as:

$$\begin{cases}\displaystyle\int_\Omega tr(\boldsymbol{\sigma}(\boldsymbol{\epsilon}(\boldsymbol{u}),\boldsymbol{H})\,\boldsymbol{\epsilon}(\boldsymbol{v}))dx=\quad f_{ext}(v)\qquad\forall\boldsymbol{v}\in P^\perp\\ \qquad\qquad\qquad\boldsymbol{u}\mid_{\Gamma_u}=\boldsymbol{u}_g\mid_{\Gamma_u}\end{cases}\tag{24}$$

Here, we assume that the vector $\boldsymbol{u}_g\in\left(W^{1,2}(\Omega)\right)^n$ and $f_{ext}\in\left[\left(W^{1,2}(\Omega)\right)^n\right]^*$ (topological dual space). f_{ext} represents the sum of the body forces and of the external forces applied on Γ_τ.

Theorem 3.7. *Let f^+ and f^- such as the ones defined in proposition 3.5. Then, there exists one unique solution of the problem (P^*).*

Proof :

The existence is simply based on the classical argument: coercivity + lower semi-continuity = existence.

Let's define the function T on $P^\perp$ by:

$$T(u)=\int_\Omega\psi(\boldsymbol{\epsilon}(\boldsymbol{u}+\boldsymbol{u}_g),\boldsymbol{H})\,dx-f_{ext}(\boldsymbol{u})\tag{25}$$

Step 1: T is well defined, bounded in the neighborhood of each element of $P^{\perp}$ and strictly convex on $P^{\perp}$. In particular, T is continuous on $P^{\perp}$.

As a consequence of the convexity of ψ, for each $v \in \left(W^{1,2}(\Omega)\right)^n$ we have:

$$\int_{\Omega} \psi\left(\boldsymbol{\epsilon}\left(\boldsymbol{v}\right), \boldsymbol{H}\right) dx \quad \leq \quad \int_{\Omega} \psi\left(0, \boldsymbol{H}\right) dx + \int_{\Omega} tr\left(\widetilde{D}_{\boldsymbol{\epsilon}} \psi\left(\boldsymbol{\epsilon}\left(\boldsymbol{v}\right), \boldsymbol{H}\right) \boldsymbol{\epsilon}\left(\boldsymbol{v}\right)\right) dx \tag{26}$$

The first term on the right side of the inequality is well defined since $H \in V_H$. Using the Lipschitz property of the operator $\widetilde{D}_{\boldsymbol{\epsilon}} \psi$ demonstrated in proposition 3.6 and the assumption on H, we can find a constant C such as:

$$\int_{\Omega} tr\left(\widetilde{D}_{\boldsymbol{\epsilon}} \psi\left(\boldsymbol{\epsilon}\left(\boldsymbol{v}\right), \boldsymbol{H}\right) \boldsymbol{\epsilon}\left(\boldsymbol{v}\right)\right) dx \leq C \int_{\Omega} \left\|\boldsymbol{\epsilon}\left(\boldsymbol{v}\right)\right\|_2 \left(1 + \left\|\boldsymbol{\epsilon}\left(\boldsymbol{v}\right)\right\|_2\right) dx \tag{27}$$

From the continuity of the operator $\boldsymbol{\epsilon}(.) = \frac{1}{2}\left(\nabla(.) + \nabla^T(.)\right)$ on $P^{\perp}$, we conclude that T is well defined and bounded in the neighbourhood of each element of $P^{\perp}$.

The convexity of ψ leads to the convexity of T. The strict convexity can be seen as follow: Let $\boldsymbol{u}_1$ and $\boldsymbol{u}_2$ from $P^{\perp}$ and $r \in (0,1)$ such $T(r\,\boldsymbol{u}_1 + (1-r)\,\boldsymbol{u}_2) = r\,T(\boldsymbol{u}_1) + (1-r)\,T(\boldsymbol{u}_2)$. We deduce $\boldsymbol{\epsilon}\left(\boldsymbol{u}_1\right) = \boldsymbol{\epsilon}\left(\boldsymbol{u}_2\right)$ almost-everywhere or simply (a.e.).

The well-known Korn's inequality provides us with:

$$\left\|\boldsymbol{u}_1 - \boldsymbol{u}_2\right\|_{W^{1,2}} \leq C \left(\int_{\Omega} \left\|\boldsymbol{\epsilon}\left(\boldsymbol{u}_1\right) - \boldsymbol{\epsilon}\left(\boldsymbol{u}_2\right)\right\|_2^2 dx\right)^{\frac{1}{2}} \tag{28}$$

where $\|.\|_{W^{1,2}}$ is the norm associated with the space $(W^{1,2}(\Omega))^n$. Thus $\boldsymbol{u}_1 = \boldsymbol{u}_2$.

Step 2: T is coercive, i.e., $T(\boldsymbol{u}) \to +\infty$ as $\|\boldsymbol{u}\|_{W^{1,2}} \to \infty$

Let f be function of $\mathcal{C}^+$. From proposition 3.1, the existence of a constant c_1 such as $f(x) \geq x + c_1$ is ensured. This implies that $\int_{-\infty}^{x} f(y)\, dy \geq \frac{x^2}{2} + c_1 x$ for each positive x.

For sake of simplification, let $\boldsymbol{K} = \boldsymbol{H}^{-\frac{1}{2}}$ and $\boldsymbol{\epsilon}(\boldsymbol{u})$ is simply denoted $\boldsymbol{\epsilon}$. We deduce that:

$$\begin{aligned} \int_{\Omega} tr\left(F^{+}\left(\boldsymbol{K}\boldsymbol{\epsilon}\boldsymbol{K}\right)\right) dx \geq \frac{1}{2} \int_{\Omega} \left\|\langle \boldsymbol{K}\boldsymbol{\epsilon}\boldsymbol{K}\rangle^{+}\right\|_2^2 dx + \\ c_1 \int_{\Omega} tr\left(\langle \boldsymbol{K}\boldsymbol{\epsilon}\boldsymbol{K}\rangle^{+}\right) dx \end{aligned} \tag{29}$$

Similarly, for some constant c_2, we have:

$$\int_{\Omega} tr\left(F^{-}\left(\boldsymbol{\epsilon}\right)\right) dx \geq \frac{1}{2} \int_{\Omega} \left\|\langle \boldsymbol{\epsilon}\rangle^{-}\right\|_2^2 dx + c_2 \int_{\Omega} tr\left(\langle \boldsymbol{\epsilon}\rangle^{-}\right) dx \tag{30}$$

On the other hand, we have:

$$\int_\Omega tr\left(\left(\boldsymbol{K}\boldsymbol{\epsilon}\boldsymbol{K}\right)^2\right)dx = \int_\Omega tr\left(\left(\left\langle \boldsymbol{K}\boldsymbol{\epsilon}\boldsymbol{K}\right\rangle^+\right)^2\right)dx + \int_\Omega tr\left(\left(\left\langle \boldsymbol{K}\boldsymbol{\epsilon}\boldsymbol{K}\right\rangle^-\right)^2\right)dx \tag{31a}$$

$$\leq \int_\Omega tr\left(\left(\left\langle \boldsymbol{K}\boldsymbol{\epsilon}\boldsymbol{K}\right\rangle^+\right)^2\right)dx + \int_\Omega tr\left(\boldsymbol{K}\left(\left\langle \boldsymbol{\epsilon}\right\rangle^-\right)^2\boldsymbol{K}\right)dx \tag{31b}$$

$$\leq \int_\Omega tr\left(\left(\left\langle \boldsymbol{K}\boldsymbol{\epsilon}\boldsymbol{K}\right\rangle^+\right)^2\right)dx + \int_\Omega tr\left(\left(\left\langle \boldsymbol{\epsilon}\right\rangle^-\right)^2\right)dx \tag{31c}$$

The first line (31a) is clear. The second line (31b) is deduced from corollary 4.27 in [38] since K is contractive, i.e., the eigenvalues of K are bounded by unity (of course almost everywhere) following the definition adopted in ([37]), and the function $h : x \mapsto \left(\langle x\rangle^-\right)^2$ is convex on $\mathbb{R}$ with $h(0) = 0$. The last line (31c) is again obtained using the fact that K is contractive.

Let $L_{\boldsymbol{K}} : (\boldsymbol{\epsilon}_1, \boldsymbol{\epsilon}_2) \mapsto \int_\Omega tr\left(\boldsymbol{K}^2\boldsymbol{\epsilon}_1\boldsymbol{K}^2\boldsymbol{\epsilon}_2\right)dx$ be the continuous bilinear function on $L^2(\Omega, \mathcal{S}_n) \times L^2(\Omega, \mathcal{S}_n)$. Given the assumption on $\boldsymbol{H}$, it is easy to see that $L_{\boldsymbol{K}}$ is coercive, i.e., $\int_\Omega tr\left(\left(\boldsymbol{K}\boldsymbol{\epsilon}\boldsymbol{K}\right)^2\right)dx = L_{\boldsymbol{K}}(\boldsymbol{\epsilon}, \boldsymbol{\epsilon}) \geq c_3 \int_\Omega tr\left(\left(\boldsymbol{\epsilon}\right)^2\right)dx$ for some strictly positive constant c_3. We conclude that strictly positive constants C_3 and C_4 exist such as:

$$\begin{aligned}\int_\Omega tr\left(F^+\left(\boldsymbol{H}^{-\frac{1}{2}}\boldsymbol{\epsilon}\boldsymbol{H}^{-\frac{1}{2}}\right)\right)dx + \int_\Omega \left(1 - \eta\left\|\boldsymbol{D}\right\|\right) tr\left(F^-\left(\boldsymbol{\epsilon}\right)\right)dx \geq \\ C_3\int_\Omega \left\|\boldsymbol{\epsilon}\right\|_2^2 dx - C_4\int_\Omega \left\|\boldsymbol{\epsilon}\right\|_2 dx\end{aligned} \tag{32}$$

Applying this to the definition of T and using the Korn inequality we may find other strictly positive constants still denoted C_3, C_4 and C_5 such as:

$$T(\boldsymbol{u}) \geq C_3\left\|\boldsymbol{u}\right\|_{W^{1,2}}^2 - C_4\left\|\boldsymbol{u}\right\|_{W^{1,2}} - C_5 \tag{33}$$

Therefore, we have $T(\boldsymbol{u}) \to +\infty$ as $\left\|\boldsymbol{u}\right\|_{W^{1,2}} \to \infty$.

Step 3: T achieves its minimum at $P^\perp$ at a unique point.

$P^\perp$ is reflexive since it is a closed subspace of the reflexive space $\left(W^{1,2}(\Omega)\right)^n$. Moreover, T is proper lower semi-continuous (since T is well defined and continuous). We deduce (see for example Corollary 3.23 in [39]) that the minimum of T is achieved for some $\boldsymbol{u}_0$. The uniqueness is a consequence of the strict convexity of T (cf. *step* 1).

Step 4: $\lim_{t\to 0}\frac{T(\boldsymbol{u}_0 + t\boldsymbol{v}) - T(\boldsymbol{u})}{t} = \int_\Omega tr(\boldsymbol{\sigma}\left(\boldsymbol{\epsilon}\left(\boldsymbol{u}_0 + \boldsymbol{u}_g\right)\right)\boldsymbol{\epsilon}\left(\boldsymbol{v}\right))dx - f\left(\boldsymbol{v}\right) = 0$

Let $g(t) = \psi\left(\boldsymbol{\epsilon}\left(\boldsymbol{u}_0 + \boldsymbol{u}_g\right) + t\boldsymbol{\epsilon}\left(\boldsymbol{u}\right), \boldsymbol{H}\right)$. g is differentiable and g' is a Lipschitz function. From proposition 3.6 we can write:

$$\left|g(t) - g(0) - g'(0)t\right| \leq M\left\|\boldsymbol{\epsilon}\left(\boldsymbol{v}\right)\right\|_2^2 t^2 \ \text{(a.e. in } \Omega) \tag{34}$$

For some constant M; Using the previous inequality we deduce the result.

Step 5: The vector $\boldsymbol{u} = \boldsymbol{u}_0 + \boldsymbol{u}_g$ is the unique solution of the problem (P^*). The uniqueness is also a consequence of the strict convexity of T (cf. *step* 1). □

The well-posedness of the problem (P^*) established above shows that any evolution of the damage variable leads to a unique solution as soon as the damage variable and the external loading satisfy the conditions of the theorem 3.7. In particular, when the domain behaves with a fixed damage state, the response is unique. This suggests to prescribe a damage evolution such as the tensor $\boldsymbol{H}$ remains bounded, except in a set with a null measure. As pointed out in the introduction, the damage evolution adopted in this work is controlled by the same relations as the ones proposed by Desmorat and investigated in detail in section 3.4. Next section focuses on the positivity of the intrinsic dissipation.

3.3. Positivity of the intrinsic dissipation

As required by the second principle of thermodynamics, the rate of energy dissipation must be non-negative to ensure the irreversibility of damage process. By definition, the rate of energy dissipation is written as the difference between the mechanical power and the variation of the Helmholtz energy under isothermal condition. Moreover, the thermodynamical consistency condition is given by the Clausius-Duhem inequality which takes the following form:

$$tr(\boldsymbol{\sigma}\dot{\boldsymbol{\epsilon}}) - \rho\dot{\psi} \geq 0 \tag{35}$$

where the time derivatives are in the sense of distributions [40]. It is noteworthy that, for practical cases, the internal variables may be smooth with respect to the time variable through an interval $[0, T]$, except in a set of points with zero measure. For instance, when suddenly the internal variables stop flowing which can occur at the unloading points, i.e., the variable $\dot{\boldsymbol{H}}$ or $\dot{\boldsymbol{D}}$ may be discontinuous at this points. For that reason, we should select the tensors $\boldsymbol{\epsilon}$ and $\boldsymbol{H}$ in appropriate spaces which take into account this feature in order to verify the above inequality. It should also be highlighted that, even if the strain tensor and the internal variables are differentiable with respect to the time variable, the Helmholtz energy ψ can be not always differentiable with respect to the time variable, in the classical sense, due to the presence of the term $\|\boldsymbol{D}\|$ which is not always differentiable with respect to $\boldsymbol{D}$.

Let $L^p((0,T),\mathcal{S}_n)$ be the space of all strongly measurable functions $X : (0,T) \longmapsto \mathcal{S}_n$ for which the norm $\|X\|_{L^p((0,T),\mathcal{S}_n)} = \left(\int_0^T \|X\|_2^p\right)^{\frac{1}{p}}$ is finite, where $1 \leq p < \infty$. For $p = \infty$, $L^\infty((0,T),\mathcal{S}_n)$ is the space of measurable functions $X : (0,T) \longmapsto \mathcal{S}_n$ such

$\|X(t)\|_2 \leq C$ (a.e.) for some constant C equipped with the norm $\|X\|_{L^\infty((0,T),\mathcal{S}_n)} = \inf\{C; \|X(t)\|_2 \leq C\,(a.e.)\}$. Similarly, let $W^{1,p}((0,T),\mathcal{S}_n)$ be the space of all measurable functions $X : (0,T) \longmapsto \mathcal{S}_n$ for which the norm $\|X\|_{W^{1,p}((0,T),\mathcal{S}_n)} = \left(\int_0^T \|X\|_2^p + \int_0^T \left\|\dot{X}\right\|_2^p\right)^{\frac{1}{p}}$ is finite, where $\dot{X}$ stands for the time derivative of X in the sense of the distribution. The following lemma, considered as a starting point to prove the positivity of the dissipation, shows that a weak assumption on the rate $\dot{\boldsymbol{H}}$ is sufficient to ensure a continuous growth of the principal damage variables.

Lemma 3.8. *Let's assume that H belongs to the space $W^{1,1}((0,T),\mathcal{S}_n)$ such as $\dot{H} \geq 0$ (a.e.). Then the eigenvalues of $\boldsymbol{D}(t)$ can be represented by continuous and non decreasing functions. In other words, non decreasing continuous functions $D_1(t)$,...,$D_n(t)$ such that, for t (a.e.), are the eigenvalues of $D(t)$ exist. Moreover, if $\boldsymbol{H}(t=0) = \boldsymbol{I}$, then the eigenvalues of $\boldsymbol{D}(t)$ belong to $[0,1]$ for all times $t \geq 0$.*

Proof :

Since $\boldsymbol{H} \in W^{1,1}((0,T),\mathcal{S}_n)$, $\boldsymbol{H}$ can be represented by a continuous function on the compact $[0,T]$ with respect to the norm $\|.\|_2$, denoted also $\boldsymbol{H}$.

Let $\left(H_i^{\downarrow}(t)\right)_{1\leq i\leq n}$ be the eigenvalues of $\boldsymbol{H}(t)$ arranged in decreasing order, i.e., $H_n^{\downarrow} \leq ... \leq H_1^{\downarrow}$. Since $\boldsymbol{H}(t)$ is Hermitian, the Weyls perturbation theorem ensures that for all $(t_1,t_2) \in [0,T]^2$:

$$\max_i \left|H_i^{\downarrow}(t_1) - H_i^{\downarrow}(t_2)\right| \leq \|\boldsymbol{H}(t_1) - \boldsymbol{H}(t_2)\| \tag{36}$$

where $\|.\|$ is the bound norm. Given the equivalence between the norms $\|.\|$ and $\|.\|_2$, the continuity of the function $H(t)$ and the norm $\|.\|$, we deduce that the functions $H_i^{\downarrow}(t)$, $1 \leq i \leq n$, are continuous using the previous equation (36).

Let's assume that $t_1 \leq t_2$, the hypotheses on $\boldsymbol{H}(t)$ allow us to write:

$$H(t_2) - H(t_1) = \int_{t_1}^{t_2} \dot{\boldsymbol{H}}(t)\,dt \geq 0 \tag{37}$$

which is equivalent to write for all $x \in \mathbb{R}^n$ such as $\|x\| = 1$:

$$\langle x, \boldsymbol{H}(t_1)x\rangle \leq \langle x, \boldsymbol{H}(t_2)x\rangle \tag{38}$$

For all i such as $1 \leq i \leq n$, the well-known Minmax principle yields:

$$H_i^{\downarrow}(t) = \max_{\substack{M\subset\mathbb{R}^n \\ dim(M)=k}} \min_{\substack{x\in M \\ \|x\|=1}} \langle x, \boldsymbol{H}(t)x\rangle \tag{39}$$

Combining the equation (39) with the inequality (38), we deduce $H_i^{\downarrow}(t_1) \leq H_i^{\downarrow}(t_2)$.

For $1 \leq i \leq n$, let $D_i(t) = 1 - \left(H_i^{\downarrow}(t)\right)^{-2}$. It is clear that $(D_i(t))_{1\leq i\leq n}$ are the eigenvalues of $\boldsymbol{D}(t)$ (a.e.) which are, according to the above results, represented by non decreasing continuous functions. Moreover, if $\boldsymbol{H}(0) = \boldsymbol{I}$, then $D_i(t)$ are positive and bounded by the unity. □

Lemma 3.9. *Let f be an operator function of class $C^1(J)$, where J is an interval. If $\boldsymbol{H} \in W^{1,1}((0,T),\mathcal{S}_n)$ such as the eigenvalues of $\boldsymbol{H}(t)$ are in J for all t then $f(\boldsymbol{H}(t)) \in W^{1,1}((0,T),\mathcal{S}_n)$ and the weak derivative is equal to $\widetilde{D}f\,(H)\left(\dot{\boldsymbol{H}}(t)\right)$. Moreover, for the couple (t_1,t_2) (a.e.) we have:*

$$f(\boldsymbol{H}\,(t_2)) - f(\boldsymbol{H}\,(t_1)) = \int_{t_1}^{t_2} \widetilde{D}f\,(\boldsymbol{H})\left(\dot{\boldsymbol{H}}(t)\right) dt \tag{40}$$

Proof :

From the The continuous differentiability of $f(.)$, it is clear that $f(X(t))$ and $\widetilde{D}f(X(t))(Y(t))$ are measurable, for all measurable functions $X(t)$ and $Y(t)$ on $(0,T)$.

Since $\boldsymbol{H} \in W^{1,1}\left((0,T),\mathcal{S}_n\right)$, then $\boldsymbol{H}(t)$ is bounded (a.e.). In this case, it is straightforward that $f(\boldsymbol{H}) \in L^1\left((0,T),\mathcal{S}_n\right)$ using the mean theorem. The continuous differentiability of $f(.)$ implies that $\widetilde{D}f(\boldsymbol{H}(.))$ is bounded on $(0,T)$ (a.e.). We deduce that $\widetilde{D}f(\boldsymbol{H})(\dot{\boldsymbol{H}}) \in L^1\left((0,T),\mathcal{S}_n\right)$.

Since $C_c^1(\mathbb{R},\mathcal{S}_n)$ is dense in $W^{1,1}\left((0,T),\mathcal{S}_n\right)$, we can choose a sequence of smooth functions that converges to $\boldsymbol{H}$ in $W^{1,1}\left((0,T),\mathcal{S}_n\right)$. Taking into account the continuous injection $W^{1,1}((0,T),\mathcal{S}_n) \subset L^{\infty}((0,T),\mathcal{S}_n)$ and the dominated convergence theorem, the result follows immediately. □

Remark Following the proof of Lemma 3.5, each element of $W^{1,1}\left((0,T),\mathcal{S}_n\right)$ can be represented by a continuous function. We can assume, henceforth, that $\boldsymbol{H}$ is continuous on $[0,T]$ but not necessary with continuous first derivative.

□

Proposition 3.10. *Let F^+, G^+, F^- and G^- be the functions defined above. Let's assume that $\boldsymbol{\epsilon} \in W^{1,1}\left((0,T),\mathcal{S}_n\right)$ and $\boldsymbol{H} \in W^{1,1}\left((0,T),\mathcal{S}_n\right) \cap C^0\left([0,T],\mathcal{S}_n\right)$. If $\dot{\boldsymbol{H}} \geq 0$ (a.e.) such $\boldsymbol{H}(0) = I$ and $f^+ = 0$ within the interval $]-\infty,0]$, then $\boldsymbol{\sigma}\dot{\boldsymbol{\epsilon}} - \rho\dot{\psi} \geq 0$.*

Proof :

In order to prove the inequality (35), it is sufficient to show that:

$$\int_0^T \left(tr(\boldsymbol{\sigma}\dot{\boldsymbol{\epsilon}}) - \rho\dot{\psi} \right) \varphi \, dt \geq 0 \quad \forall \varphi \in \mathcal{D} = C_c^\infty \left((0,T) \right) \quad \varphi \geq 0 \tag{41}$$

It is clear that $\int_0^T tr(\boldsymbol{\sigma}\dot{\boldsymbol{\epsilon}})$ is well defined since $\boldsymbol{\sigma} \in L^\infty((0,T),\mathcal{S}_n) \cong \left(L^1 \left((0,T), \mathcal{S}_n \right) \right)^*$, following the definition (19) and the continuous injection $W^{1,1}((0,T),\mathcal{S}_n) \subset L^\infty((0,T),\mathcal{S}_n)$.

The relation $\boldsymbol{D} = \boldsymbol{I} - \boldsymbol{H}^{-2}$ is well defined since $\dot{\boldsymbol{H}} \geq 0$ and $\boldsymbol{H}(0) = \boldsymbol{I}$. Lemma 3.9 and the continuity of H show that $\boldsymbol{D} \in W^{1,1} \left((0,T), \mathcal{S}_n \right)$. Moreover, $t \longmapsto \|\boldsymbol{D}(t)\|$ is absolutely continuous, given that $| \, \|\boldsymbol{D}(t_2)\| - \|\boldsymbol{D}(t_1)\| \, | \leq \|\boldsymbol{D}(t_2) - \boldsymbol{D}(t_1)\| \leq \int_{t_1}^{t_2} \left\| \dot{\boldsymbol{D}} \right\| \, dt$, we conclude that the function $t \longmapsto \|\boldsymbol{D}(t)\|$ has a pointwise defined (a.e.) derivative which is integrable on $(0,T)$. Moreover, the eigenvalues of $\boldsymbol{D}$ are non decreasing with respect to the time (in the sense of the representations) provided that $\dot{\boldsymbol{H}}$ remains positive (a.e.) as stated in lemma 3.8. Thus, the derivative of $\|\boldsymbol{D}(t)\|$ is positive, i.e., $\int_0^T \frac{d\|\boldsymbol{D}\|}{dt}\varphi = \lim_{h\to 0} \int_0^T \frac{\|\boldsymbol{D}(t+h)\| - \|\boldsymbol{D}(t)\|}{h}\varphi \geq 0$.

The integral $\int_0^T \rho\psi\dot{\varphi}$ is well defined. It can be shown that, in the sense of distributions, we have $\left\langle \dot{\psi}, \varphi \right\rangle_{\mathcal{D}^*,\mathcal{D}} = \int_0^T \dot{\psi}\varphi dt$. Indeed, it is sufficient to assume that $\boldsymbol{H}$ and $\boldsymbol{\epsilon}$ are differentiable with respect to the time in the classical sense, then we conclude by density argument and the dominated convergence theorem using the continuity feature of the cracking functions. Using this last argument and the relation (19), we end up with the following development:

$$\int_0^T \left(tr(\boldsymbol{\sigma}\dot{\boldsymbol{\epsilon}}) - \rho\dot{\psi} \right) \varphi dt = -\rho \int_0^T \left(\widetilde{D}_{\boldsymbol{H}} \psi^+_{F^+,G^+} \left(\boldsymbol{\epsilon}, \boldsymbol{H} \right) \left(\dot{\boldsymbol{H}} \right) - \eta \frac{d\,\|\boldsymbol{D}\|}{dt} \right) \varphi \, dt \tag{42}$$

each term of the above integral can be written as:

$$\int_0^T \widetilde{D}_{\boldsymbol{H}} tr \left(F^+ \left(\boldsymbol{H}^{-\frac{1}{2}} \boldsymbol{\epsilon} \boldsymbol{H}^{-\frac{1}{2}} \right) \right) \left(\dot{\boldsymbol{H}} \right) \varphi dt = - \int_0^T tr \left(\boldsymbol{H}^{-\frac{1}{2}} h \left(\boldsymbol{H}^{-\frac{1}{2}} \boldsymbol{\epsilon} \boldsymbol{H}^{-\frac{1}{2}} \right) \boldsymbol{H}^{-\frac{1}{2}} \dot{\boldsymbol{H}} \right) \varphi dt \tag{43}$$

and:

$$\int_0^T \widetilde{D}_{\boldsymbol{H}} \frac{1}{tr\left(\boldsymbol{H}^2\right)} \left(\dot{\boldsymbol{H}} \right) \varphi \, dt = -2 \int_0^T \frac{tr(\boldsymbol{H}\dot{\boldsymbol{H}})}{\left(tr\left(\boldsymbol{H}^2\right) \right)^2} \varphi \, dt \tag{44}$$

where h is the operator function defined by $h : x \longmapsto x f^+(x)$, which is non-negative. From the assumptions on the tensor $\boldsymbol{H}$ we conclude that $\int_0^T \left(tr(\boldsymbol{\sigma}\dot{\boldsymbol{\epsilon}}) - \rho\dot{\psi} \right) \varphi \, dt \geq 0$ using the equivalence property and Fejer's theorem.

□

3.4. Damage evolution

Generally, the damage evolution law is classically ensured by the normality rule, such as the damage rate belongs to the normal cone of a convex set bounding the elastic domain. The initial Desmorat's model [41] uses simply the hyperplane to define the elastic domain as $\Phi(\boldsymbol{D}) = tr\left(\boldsymbol{D}(\langle\boldsymbol{\epsilon}\rangle^{+})^{\alpha}\right)$, where α is a damage exponent. Thus, the evolution law reads $\dot{\boldsymbol{D}} = \dot{\lambda}\,(\langle\boldsymbol{\epsilon}\rangle^{+})^{\alpha}$. The last version of the model [8] is based upon a flow rule of the form $\dot{\boldsymbol{H}} = \dot{\lambda}\,\langle\tilde{\boldsymbol{\epsilon}}\rangle^{+}$, where $\langle\tilde{\boldsymbol{\epsilon}}\rangle^{+}$ is the effective strain. Despite the fact that both relations lead to a non decreasing damage principal variables in the sense of the representations discussed in lemma 3.8, it should be pointed out there is no equivalence between the positivity of the tensor rates when they are sufficiently smooth. Indeed, we claim:

Lemma 3.11. *Let's consider $\phi = (\boldsymbol{I} - \boldsymbol{D})^{p}$, where $-1 < p < 0$ then the positivity of the rate $\dot{\boldsymbol{D}}$ implies the positivity of the rate $\dot{\phi}$. The converse is not true.*

Proof :

It is sufficient to prove that if $\boldsymbol{D}_1 > \boldsymbol{D}_2$ then $\phi(\boldsymbol{D}_1) > \phi(\boldsymbol{D}_2)$. Indeed, we have $\boldsymbol{I} - \boldsymbol{D}_1 < \boldsymbol{I} - \boldsymbol{D}_2$ and $x \longmapsto x^{-p}$ is a monotone operator function (see [37]), then $(\boldsymbol{I} - \boldsymbol{D}_1)^{-p} < (\boldsymbol{I} - \boldsymbol{D}_2)^{-p}$ and $(\boldsymbol{I} - \boldsymbol{D}_1)^{p} > (\boldsymbol{I} - \boldsymbol{D}_2)^{p}$. The converse is not true. In fact, let's $h : x \longmapsto (1+x)^{-\frac{1}{p}}$ defined on the real line $[0, +\infty[$. h cannot be a monotone operator function since h is not concave (see theorem V.2.5 [37]), then positive tensors A_1 and A_2 such as $A_1 > A_2$ and $(I + A_1)^{-\frac{1}{p}} \not\geq (I + A_2)^{-\frac{1}{p}}$ exist. Let's be $\phi_1 = (I + A_1)$ and $\phi_2 = (I + A_2)$ and $\phi(t) = (1-t)\phi_2 + t\phi_1$ for $0 \leq t \leq 1$. It is clear that $\dot{\phi} \geq 0$ but $\dot{\boldsymbol{D}} \not\geq 0$ because $\boldsymbol{D}(t=1) \not\geq \boldsymbol{D}(t=0)$. □

In this work, the damage evolution is governed, almost, by the same equations as the ones proposed in [8, 41]. Indeed, the integrity tensor rate $\dot{\boldsymbol{H}}$ is proportional to the positive part of the real strain tensor instead of the positive part of the effective strain tensor, as suggested in [8]. The damage criterion is given by:

$$f = \hat{\epsilon} - \kappa \leq 0 \tag{45}$$

where $\hat{\epsilon} = \sqrt{tr\left(\langle\boldsymbol{\epsilon}\rangle^{+}\langle\boldsymbol{\epsilon}\rangle^{+}\right)}$ is the Mazars's equivalent strain [42] and κ is called the consolidation function which is linear with respect to $tr(\boldsymbol{H})$:

$$\kappa = \kappa_0 + SR_{\nu}^{s}\,(tr(\boldsymbol{H}) - 3) \tag{46}$$

Here, κ_0 is the damage threshold, S the damage strength and s the triaxiality exponent. The triaxiality function R_ν is written in term of the stress triaxiality T_X and bounded by a material constant B as follows:

$$R_\nu = \min\left[1 + 8\frac{1-2\nu}{1+\nu}\left\langle -T_X\right\rangle^2,\ B\right] \quad T_X = \frac{tr(\boldsymbol{\sigma})}{3\,\sigma_{eq}} \tag{47}$$

where σ_{eq} is the von Mises equivalent strain.

3.5. Numerical implementation

The integration procedure is quite simple and follows the same steps as the ones proposed by Desmorat in [8] without the need to compute the effective strain and the effective stress tensors. The time discretization of the damage evolution equation is performed using an Euler explicit scheme. One can summarize the integration process in Algorithm 1.

Algorithm 1: Time integration algorithm to compute the stress tensor $\boldsymbol{\sigma}_n$

Input : strain tensor $\boldsymbol{\epsilon}_n$, equivalent strain $\hat{\epsilon}_n = \left\|\left\langle \boldsymbol{\epsilon}_n\right\rangle^+\right\|_2$, κ_{n-1}, $R_{\nu,n-1}$ and $\boldsymbol{D}_{n-1}$

Output: $\boldsymbol{\sigma}_n$, $\boldsymbol{D}_n$ and $R_{\nu,n}$

$\boldsymbol{H}_{n-1} = (\boldsymbol{I} - \boldsymbol{D}_{n-1})^{-\frac{1}{2}}$;

$\boldsymbol{H}_n = \boldsymbol{H}_{n-1}$;

if $f = \hat{\epsilon}_n - \kappa_{n-1} \leq 0$ **then**

| $\triangle\lambda = 0$;

else

| $tr(\boldsymbol{H}_n) = 3 + \frac{\hat{\epsilon}_n - \kappa_0}{SR^s_{\nu,n-1}}$;

| $\triangle\lambda = \frac{tr(\boldsymbol{H}_n) - tr(\boldsymbol{H}_{n-1})}{tr\left(\langle\boldsymbol{\epsilon}_n\rangle^+\right)}$;

| $\kappa_n = \hat{\epsilon}_n$;

end

$\boldsymbol{H}_n = \boldsymbol{H}_{n-1} + \Delta\lambda\left\langle\boldsymbol{\epsilon}_n\right\rangle^+$;

$\boldsymbol{D}_n = \boldsymbol{I} - \boldsymbol{H}_n^2$;

$\boldsymbol{\sigma}_n^+ = 2\mu\,\boldsymbol{H}_n^{-\frac{1}{2}} f^+\left(\boldsymbol{H}_n^{-\frac{1}{2}}\boldsymbol{\epsilon}_n\boldsymbol{H}_n^{-\frac{1}{2}}\right)\boldsymbol{H}_n^{-\frac{1}{2}} + \lambda\,\frac{3}{tr(\boldsymbol{H}_n^2)}\,g^+\left(tr\left(\boldsymbol{\epsilon}_n\right)\right)\,\boldsymbol{I}$;

$\boldsymbol{\sigma}_n^- = 2\mu\left(1 - \eta\left\|\boldsymbol{D}_n\right\|\right)\,f^-\left(\boldsymbol{\epsilon}_n\right) + \lambda\,g^-\left(tr\left(\boldsymbol{\epsilon}_n\right)\right)\boldsymbol{I}$;

$\boldsymbol{\sigma}_n = \boldsymbol{\sigma}_n^+ + \boldsymbol{\sigma}_n^-$;

$T_{X,n} = \frac{tr(\boldsymbol{\sigma}_n)}{3\,\sigma_{eq,n}}$;

$R_{\nu,n} = \min\left[1 + \frac{9}{2}\frac{1-2\nu}{1+\nu}\left\langle -T_{X,n}\right\rangle^2,\ B\right]$;

With the aim to control the mesh dependency effects, an integral nonlocal regularization approach ([43, 44]) is adopted to ensure numerical convergence to physical solutions. In the following, the approach adopted in [43] is used and consists in substituting the local equivalent strain by its nonlocal value obtained by averaging over the space domain as follow:

$$\hat{\epsilon}^{eq}(x) = \frac{1}{V_r(x)} \int_V \alpha_0 \left(\frac{\|x-\xi\|}{l_c} \right) \hat{\epsilon}(\xi)\, d\xi \tag{48}$$

where $V_r(x)$ is given by:

$$V_r(x) = \int_V \alpha_0 \left(\frac{\|x-\xi\|}{l_c} \right) d\xi \tag{49}$$

The quantity V_r is the representative volume and plays the role of a normalizing coefficient. The function α_0 is called the nonlocal weight function which often selected to be the Gaussian function $\alpha_0(\xi) = \exp\left(-\frac{1}{2}\xi^2\right)$ or bell shaped function [45]. l_c is the characteristic length, generally assumed to be correlated with the aggregate size following the relation $l_c \approx 3d_a$, where d_a is the maximum aggregate size (see for instance [46]). Others studies have reported the relation $l_c = 8\,mm$ [47] or use only $l_c = 1.1\,mm$ [48]. Thereafter, the criterion function is substituted by:

$$f = \hat{\epsilon}^{eq} - \kappa \leq 0 \tag{50}$$

4. Numerical examples

In order to assess the numerical robustness of the proposed model, several tests are carried out using different cracking functions satisfying the conditions mentioned in section 3.1 with less or more regularity properties. In this work, three different opening cracking functions f_1^+, f_2^+ and f_3^+ are considered:

$$\begin{cases} f_1^+(x) = \max(0, x) \\ f_2^+(x) = \max\left(0, x\exp\left(-\dfrac{c_1}{x}\right)\right) \\ f_3^+(x) = \dfrac{1}{c_2}\ln\left(1+\exp(c_2 x)\right) \end{cases} \tag{51}$$

where c_i $i \in \{1, 2\}$ are positive constants. It can be checked that the smooth functions (f_2^+ and f_3^+) are convex by studying the sign of the second derivative. Moreover, the functions f_2^+ and f_3^+ are infinitely differentiable in the neighborhood of 0, unlike the function f_1^+, leading to a smooth recovering of stiffness. It is interesting to notice that

the functions f_2^+ and f_3^+ converge pointwise to f_1^+ when the parameters c_1 and c_2 are close to 0 and infinity, respectively. Similarly, we define three closure cracking functions f_1^-, f_2^- and f_3^- as:

$$\begin{cases} f_1^-(x) = \min(0, x) \\ f_2^-(x) = \min\left(0, x\exp\left(\dfrac{c_1}{x}\right)\right) \\ f_3^-(x) = -\dfrac{1}{c_2}\ln(1 + \exp(-c_2 x)) \end{cases} \tag{52}$$

4.1. Uniaxial loading path

The first example concerns the classical uniaxial test by considering one multilinear cubic element of the size equal to the unity. The mechanical properties are selected close the those adopted in [8], such as: the Young's modulus $E = 36000\ MPa$, the Poisson's ratio $\nu = 0.2$, damage threshold $\kappa_0 = 5 \times 10^{-5}$, the damage strength $S = 1 \times 10^{-4}$, the triaxiality exponent $s = 5$, and the material constant $B = \frac{5}{3}$. The parameters c_i have to be chosen in such a way that the cracking functions are sufficiently close to the line $x \longmapsto x$, up to a constant. They are chosen such as $c_1 = 10^{-5}$, $c_2 = 10^4$.

In figure 1(a), the response under tension and compression are shown. We can notice that the results are consistent with the experimental evidences, in particular, the responses exhibit a softening behavior with asymmetry between tension and compression. The failure surface is plotted in Figure 1 (b). It is worth noticing that the same curve would have been obtained using the Desmorat's model, since the damage criterion, in the proposed model, remains unchanged (see section 3.4) and the new model behaves approximately linearly close to the peak stresses.

[Figure 1 about here.]

The effect of the regularity is shown in Figure 2, for $\eta = 0.5$. The non regular case is obtained by selecting $f^+ = f_1^+$, $g+ = f_3^+$, $f^- = f_1^-$ and $g^- = f_3^-$ whereas the regular case is obtained by selecting $f^+ = f_2^+$, $g^+ = f_3^+$, $f^- = f_2^-$ and $g^- = f_3^-$. During the elastic undamaged stage, the behavior is clearly non linear due to the nature of the used cracking functions. Moreover, the regular functions bring smoothness in the response with residual strains when unloading, whereas the non regular functions exhibit an abrupt change of the slope.

As depicted in Figure 3(a), when the parameter η is modified using the proposed regular functions with $c_1 = 10^{-5}$ $c_2 = 7 \times 10^3$, it is seen that the stiffness recovery is influenced by the parameter η . As expected, the secant modulus is totally recovered

for $\eta = 0$ and partially recovered for $\eta = 0.5$ and $\eta = 1$. Moreover, the fact that the brittleness increases with η may be expected since the stiffness is further weakened in the directions where the compressive strains are activated. The effect of the constant c_2 is shown in Figure 3 (b) using only $\eta = 0.5$. One can notice that the residual strains increase when the parameter c_2 decreases. Heuristically, this can be explained by the fact that the coefficient associated with the function g^-, in the equation (19), becomes more significant than the coefficient associated with the function g^+ when the damage is activated. As consequence, the normal stress needed to "close the crack", i.e., $\boldsymbol{\epsilon} \approx 0$, is of order $-\frac{\ln(2)\lambda}{c_2}\left(1 - \frac{3}{tr(\boldsymbol{H}^2)}\right) < 0$, which decreases in magnitude with c_2 and increases in magnitude with the damage (see also Figure 4). The fact that the irreversible strains increase with the damage is an interesting feature that matches with the experimental observations (see for instance [33]).

[Figure 2 about here.]

[Figure 3 about here.]

[Figure 4 about here.]

The effectiveness of the regularized nonlocal approach following the nonlocal field function (48) is tested on an elementary tensile failure problem of a three-dimensional straight bar of length $L = 4m$ with uniform mesh as illustrated in Figure 5 (a). The bar is splitted into finite number of 8-node hexahedron elements with three different meshes: Nel=21, 42 and 84, where Nel denotes the number of the elements along the bar. In order to concentrate the damage at the middle of the beam, the Young's modulus of the elements located at the middle have been weakened 100 times. Figures 5 (b) and (c) shows the load-displacement curves and the damage profiles along the bar for the three meshes using a particular value of the characteristic length $l_c = 0.2m$. It is seen that the different curves are almost close which means that the nonlocal approach minimize the spurious effects due to the mesh dependency. Moreover, It is seen that the curves associated with the medium (Nel=42) and fine (Nel=84) meshes coincide comparing with the coarse mesh (Nel=21) which means that the solution seems to converge as long as the mesh is refined.

[Figure 5 about here.]

4.2. Pure distorsion

Regarding the case of a pure distortion loading, the results obtained by the proposed model are illustrated in Figure 6 using this family of cracking functions: $f^+ = f_2^+$,

$g^+ = f_3^+$, $f^- = f_2^-$ and $g^- = f_2^-$with the following parameters: $E = 36000\ MPa$, $\nu = 0.2$, $\kappa_0 = 5 \times 10^{-5}$, $S = 1 \times 10^{-4}$, $s = 5$, $B = \frac{5}{3}$, $c_1 = 10^{-10}$ and $c_2 = 3 \times 10^4$. Despite the fact that the responses are quite different with respect to η, it is easy to check that each curve follows an asymptote characterized by a positive slope equal to $(1 - \eta)\mu$, when the strain increases indefinitely. Especially, the case $\eta = 1$ leads to softening behavior with indefinitely decreasing stresses while the other cases exhibit softening at the beginning but, sooner or later, the stress stops increasing. Equivalent results, for the cases $\eta < 1$, have been observed by Carol *et al.* following their proposed anisotropic model [27]. According to the same authors, this behavior can be explained, from a physical point of view, by the fact that the increase of compression exceeds the decrease in tension since the damage is only developed in one direction [28] (like in the present model). The last case $\eta = 1$ exhibits a different behavior compared with the previous cases but which is similar to the majority of the anisotropic (or isotropic) damage models proposed in the literature. Because of the lack of experimental results, it is difficult to decide which of the previous responses is the right one, i.e., with softening or hardening.

Paying attention to cyclic loading, the results are shown in Figure 7 with restriction to the case $\eta = 1$. It is observed that the stiffness is almost completely recovered when the direction of loading is reversed after the first softening stage. This result can not be obtained using isotropic models for which the slope is unchanged after the inversion of the sign of the loading. For this particular loading case, it can be verified that the damage and the strain tensor have the same eigenvectors due to the proportionality relation entailing that the first principle damage variable D_1 grows while the second D_2 remains equal to zero during the first loading stage. The roles are reversed when the strain flows in the negative direction except that D_1 is constant but no more equal to zero.

[Figure 6 about here.]

[Figure 7 about here.]

4.3. Willam's test

Unlike isotropic damage models, it is well-known that anisotropic models no longer ensure that the principal directions between the stress and the strain tensors are the same when the damage starts flowing. In order to investigate this effect, the plane stress problem proposed by Willam *et al.* is considered following two loading stages. The first step consists in applying tensile strain in the x-direction combined with lateral contraction in the y-direction in the proportions (1, ν) when the peak of the uniaxial stress-strain

law is reached, combination of strain components ϵ_{zz}, ϵ_{xx} and ϵ_{xz} are prescribed in the proportions (0.5, 0.75, 1).

The parameters adopted in this example are: $E = 36000\ MPa$, $\nu = 0.2$, $\kappa_0 = 8{\times}10^{-5}$, $S = 5{\times}10^{-5}$, $s = 5$ and $B = \frac{5}{3}$. Figure 8 (a) illustrates the evolution of the different stress components using regular functions with $\eta = 1$, $c_1 = 10^{-10}$ and $c_2 = 10^4$. Before reaching the peaks, the normal stress responses are elastic. It is observed that the component σ_{xx} exceeds σ_{zz} at some point during the softening response whereas the shear stress evolves with negative values after a small positive peak with respect to the other components. The response of isotropic models would be very different regarding the two previous aspects as observed by Carol *et al.* in [28], i.e., the shear stress keeps on evolving with positive value and the component σ_{xx} remains always below the evolution of σ_{zz}.

The evolution of the principal direction angles θ_ϵ, θ_σ and $\theta_{\boldsymbol{D}}$ associated with the strain, the stress and the damage tensors, respectively, are shown in Figure 8 (b). It is seen that the rotation of the damage principle directions follows the ones of the strain tensor with a slight difference while the rotation of the stress principal directions is widely significant. It is interesting to emphasize that similar results have been reported by Carol *et al.* in [28]. A similar gap seems to be related primarily to the fact the stress is recovered by the principal axis that correspond to the stiffer part.

[Figure 8 about here.]

4.4. Single edge notched concrete beam

The following test is the three-point bending test. It is carried out using a beam with a square cross section with height $a = 0.07$ cm and length equal to $4a$. The beam is characterized by a Young modulus $E = 36000\ MPa$ and a Poisson's ratio $\nu = 0.2$. The other parameters are chosen as follow: $\kappa_0 = 8 \times 10^{-5}$, $S = 9 \times 10^{-5}$, $s = 5$, $B = \frac{5}{3}$, $c_1 = 10^{-10}$ and $c_2 = 3{\times}10^4$. A notch of depth $\frac{a}{2}$ and thickness $e = 3\,mm$ has been added in the middle of the specimen. Progressive displacement is prescribed at the upper center of the beam with one cycle. The aims is to check whether the model is able to recover the stiffness when the cracks close.

The numerical analysis is carried out using a plane stress assumption. Figure 9 (a) illustrates the mesh that is composed of linear triangular elements of the size varying from 1 mm to 10 mm. The finite element solution is computed using the non local strategy, using $l_c = 3$ mm to avoid the spurious mesh-dependent effects.

[Figure 9 about here.]

[Figure 10 about here.]

Figure 9 (b) illustrates the response for two different values of η. First, it is seen, as expected, that the brittleness increases while the peak load decreases with η. Secondly, the effect of initial micro-cracks are represented by a nonlinear stage at the pre peak regime. In both cases, irreversible strains are introduced and the stiffness is recovered with a smooth transition as desired when the loading switches from tension to compression. As expected, the full recovery is obtained for the case $\eta = 0$, where slope almost equal to the initial one. Contours of the different components of the damage tensors are shown in Figure 10 at the maximum damage state. From a quantitative point view, the component D_{11} describing microcracks density caused by tensions direction 1 is more significant compared with other components. Especially, the component D_{12} is too small. This shows that the crack paths are mainly developed in directions 1 and 2.

4.5. Tensile test for double edge notched concrete specimen

The above developments are also validated in case of a tensile test carried out on a double edge notched specimen, as described in [49] where the off-set value is restricted to 10 mm. The mesh, depicted in Figure 11, is composed of 1228 linear triangular elements with a minimum size mesh equal to 1 mm. The characteristic length is $l_c = 2$ mm and the thickness of the specimen is taken to be equal to 10 mm. The following test consists in prescribing a displacement on the top of the specimen while the bottom edge is fixed. The material properties are: $E = 36000\ MPa$, $\nu = 0.2$, $\kappa_0 = 1 \times 10^{-4}$, $S = 1.3 \times 10^{-4}$, $s = 5$, $B = \frac{5}{3}$, $c_1 = 10^{-10}$ and $c_2 = 3 \times 10^4$.

[Figure 11 about here.]

[Figure 12 about here.]

The load/displacement curves are presented in Figure 11 (b) for different values of η. Similarly to the previous example, the softening increases with the parameter η and the irreversible strains are introduced. Moreover, it is seen that the initial stiffness slope is completely or partially recovered with smooth transition according to the choice of η. Once again, the damage contours, plotted in Figure 12, show that the predominant cracks appear in the direction 2, where the patterns are similar to the experimental ones discussed in the reference [50]. Finally, we should stress that using the iterative solver with updating the secant stiffness has improved the computational cost 10 times, i.e., the CPU time is reduced 10 times, comparing with the classical iterative solver (without updating the secant stiffness).

5. Conclusions

A class of damage models based upon the second order integrity tensor has been developed by means of family of functions called here opening (closure) cracking functions. The unilateral effect is taken into account by a split between the damaged part and the undamaged (or partially damaged) part, where the transition between open and close cracking state could be smoothed using the cracking functions. The model has also the property to introduce irreversible strains during the unloading regime. As required by the thermodynamic principles, the positivity of the intrinsic dissipation has been demonstrated rigorously. The Clausius-Duhem inequality is satisfied in the sense of distributions.

A well posedness result has also been established, for a given damage state where the damage tensor should be strictly bounded by unity, in the sense of the bound norm, in the whole domain except in a set of zero measure. The relationship between the integrity tensor rate and the damage tensor rate has been analyzed. It turns out that no equivalence between the rate positivity can be established for a wide class of integrity tensors frequently used in the literature. Despite this drawback, it has been shown that the damage principle values could be represented by non decreasing positive functions, strictly bounded by unity provided that the integrity tensor satisfies some weak positivity assumptions. The damage flow rule proposed by Desmorat has been adopted in this work which satisfy all the requirements cited above. The time integration procedure is similar to the one that proposed by Desmorat. Its implementation does not require to iterate in order to compute the multiplier associated with damage rate. The nonlocal approach has also been introduced to limit the mesh dependency effects.

Numerical examples have been performed to demonstrate the robustness of the model. The dissymmetry between tension and compression behaviors has been highlighted using the uniaxial test. The pure distortion test has shown that the stiffness is almost recovered when the load is switched from one direction to the opposite one. The Willam's test exhibits similar results to the ones obtained in the work of Carol *et al.*. The last tests carried out on the notched specimens have shown qualitative results which are similar to that observed during the experiments.

Although the dissymmetry between tension and compressive is well represented, it should be stressed that the behavior under the compressive strain, for a cyclic tension-compression test, still depends on the loading history in the tension direction due to the adopted flow rule. A suggested improvement will be to consider the active damage

strategy (Souid *et al.*, 2009). Future works will also focus on the calibration of the model's parameters by considering reinforced structures under cyclic loading and mixed mode tests such as Nooru-Mohamed test.

Acknowledgement

The authors wish to express their most grateful thanks to CEA/DEN for its financial support. The work carried out under the SINAPS@ project has benefited from French funding managed by the National Research Agency under the program Future Investments (SINAPS@ reference No. ANR-11-RSNR-0022). The work reported in this paper has also been supported by the SEISM Institute (http://www.institut-seism.fr). We thank Professor Rodrigue Desmorat for assistance and precious comments that improved the manuscript.

Appendix A

A general quadratic form of the elastic potential coupled with anisotropic damage proposed by Ladevèse [16] for composite materials can be written in term of stress tensor $\boldsymbol{\sigma}$ using four damage variable $\boldsymbol{H}_1 = (\boldsymbol{I} - \boldsymbol{D}_1)^{\frac{1}{2}}$, $\boldsymbol{H}_2 = (\boldsymbol{I} - \boldsymbol{D}_2)^{\frac{1}{2}}$ (Ladevèse's tensor) and d_1, d_2 (scalar) as:

$$a_1 tr\left(\boldsymbol{H}_1\boldsymbol{\sigma}^+\boldsymbol{H}_1\boldsymbol{\sigma}^+ + \boldsymbol{H}_2\boldsymbol{\sigma}^-\boldsymbol{H}_2\boldsymbol{\sigma}^-\right) + a_2 tr\left(\frac{\left(\langle\boldsymbol{\sigma}\rangle^+\right)^2}{1-d_1} + \frac{\left(\langle\boldsymbol{\sigma}\rangle^-\right)^2}{1-d_2}\right) \tag{53}$$

Here, the tensor $\boldsymbol{\sigma}^+$ ($\boldsymbol{\sigma}^-$), called the special positive (negative) part of $\boldsymbol{\sigma}$, is built using the eigenvectors and the positive part of eigenvalues of the tensor $\boldsymbol{H\sigma}$ which is of course diagonalisable [16]. In addition, we can show that the relation (53) can be expressed by other means using solely the positive and the negative part functions. In fact, the tensor $\boldsymbol{H\sigma} = \boldsymbol{H}^{\frac{1}{2}}\boldsymbol{H}^{\frac{1}{2}}\boldsymbol{\sigma}$ is similar to $\boldsymbol{H}^{\frac{1}{2}}\boldsymbol{\sigma}\boldsymbol{H}^{\frac{1}{2}}$ (AB and BA are similar for all tensors A and B), given the positivity of $\boldsymbol{H}$ (not necessary positive definite) and the symmetry of $\boldsymbol{\sigma}$. Using the similarity property, one can notice that:

$$tr\left(\boldsymbol{H}_1\boldsymbol{\sigma}^+\boldsymbol{H}_1\boldsymbol{\sigma}^+\right) = tr\left(\left(\left\langle\boldsymbol{H}_1^{\frac{1}{2}}\boldsymbol{\sigma}\boldsymbol{H}_1^{\frac{1}{2}}\right\rangle^+\right)^2\right) \tag{54}$$

and:

$$tr\left(\boldsymbol{H}_2\boldsymbol{\sigma}^+\boldsymbol{H}_2\boldsymbol{\sigma}^+\right) = tr\left(\left(\left\langle\boldsymbol{H}_2^{\frac{1}{2}}\boldsymbol{\sigma}\boldsymbol{H}_2^{\frac{1}{2}}\right\rangle^+\right)^2\right) \tag{55}$$

Therefore, we can observe that the model is also built by means of the equivalent stress tensor $\boldsymbol{\sigma_H} = \boldsymbol{H}^{\frac{1}{2}}\boldsymbol{\sigma}\boldsymbol{H}^{\frac{1}{2}}$ and a specific set of the cracking functions making some similarities with the model developed in this paper. However, the Ladevèse's model is considered inappropriate to predict the behavior of monolithic materials, such as concrete material, subjected to one damage mechanism [17] for which a single damage variable has to be used.

Appendix B

Proof of proposition 3.5:

Step 1: Let $x > 0$, then for real y, we have $F^+(\frac{x+y}{2}) < \frac{F^+(x)+F^+(y)}{2}$. Similarly, if $x < 0$ then for each real y we have $F^-(\frac{x+y}{2}) < \frac{F^-(x)+F^-(y)}{2}$.

Indeed, if $0 < x < y$, the result is obvious using the convexity of F^+. Since F^+ is convex we have for each real x_1 such $x_1 < x$: $f^+(x_1) \leq \frac{F^+(x)-F^+(x_1)}{x-x_1}$. If the equality holds, then there exists (using the mean value theorem) a real $x_0 \in I = (x_1, x)$ such $f^+(x_1) = f^+(x_0)$. Given the monotony of f^+, we have $f^+(x_1) = f^+(y)$ for all $y \in [x_1, x_0]$. Let $x_2 < x_1$, such that $x_1 = tx_2 + (1-t)x_0$ for $0 < t < 1$, then by the convexity of f^+, we have $f^+(x_1) \leq \frac{1}{2}(f^+(x_2) + f^+(x_0))$ which means $f^+(x_1) \leq f^+(x_2)$. But $x_2 < x_1$ and $f^+(x_2) \leq f^+(x_1)$ then $f^+(x_1) = f^+(x_2) = f^+(y)$ for all $y \in [x_2, x_0]$. Taking x_2 to $-\infty$, we get $f^+(x_1) = 0$ and, hence, $F^+(x) = F^+(x_1)$. This is absurd since F^+ is strictly monotone on $\mathbb{R}^+$. Thus $f^+(x_1) < \frac{F^+(x)-F^+(x_1)}{x-x_1}$. Put $x_1 = \frac{x+y}{2}$, we have also $f^+(x_1)(y - x_1) \leq (F^+(y) - F^+(x_1))$. Summing the two previous inequalities, we obtain the result. The case related to F^- is proved by analogy.

Step 2: In the following, we use the terminology matrix instead of tensor. The purpose of this step is to proof that if $\boldsymbol{A}$ and $\boldsymbol{B}$ are symmetric matrices such as $\psi(\frac{\boldsymbol{A}+\boldsymbol{B}}{2}) = \frac{\psi(\boldsymbol{A})}{2} + \frac{\psi(\boldsymbol{B})}{2}$, then $\boldsymbol{A} = \boldsymbol{B}$.

First, let us observe that the convexity of the functions involved in the potential imposes that $tr(F^+(\frac{\boldsymbol{K}(\boldsymbol{A}+\boldsymbol{B})\boldsymbol{K}}{2})) = \frac{1}{2}(tr(F^+(\boldsymbol{KAK})) + tr(F^+(\boldsymbol{KBK})))$ and $tr(F^-(\frac{\boldsymbol{A}+\boldsymbol{B}}{2})) = tr(\frac{F^-(\boldsymbol{A})}{2}) + tr(\frac{F^-(\boldsymbol{B})}{2})$ since $(1 - \eta\|\boldsymbol{D}\|) > 0$ by the relation between $\boldsymbol{H}$ and $\boldsymbol{D}$, where $\boldsymbol{K} = \boldsymbol{H}^{-\frac{1}{2}}$ (note that the matrix $\boldsymbol{K}$ is positive definite).

Let $\{e_1, ..., e_n\}$ be an orthonormal basis consisting on eigenvectors of $\frac{\boldsymbol{A}+\boldsymbol{B}}{2}$ and $\lambda_{AB} = (\lambda_{AB}^{(1)}, ..., \lambda_{AB}^{(n)})$ are the associated eigenvalues arranged in nondecreasing order. Then, we have:

$$
\begin{aligned}
tr(F^-(\frac{\boldsymbol{A}+\boldsymbol{B}}{2})) &= \sum_i F^-\left(\left\langle e_i, \frac{\boldsymbol{A}+\boldsymbol{B}}{2} e_i \right\rangle\right) && \text{(56a)}\\
&\leq \sum_i \frac{1}{2}\left(F^-(\langle e_i, \boldsymbol{A}e_i\rangle) + F^-(\langle e_i, \boldsymbol{B}e_i\rangle)\right) && \text{(56b)}\\
&\leq \sum_i \frac{1}{2}\left(\langle e_i, F^-(\boldsymbol{A})\, e_i\rangle + \langle e_i, F^-(\boldsymbol{B})\, e_i\rangle\right) && \text{(56c)}\\
&= \frac{1}{2}\left(tr\left(F^-(\boldsymbol{A})\right) + F^-(\boldsymbol{B})\right) && \text{(56d)}
\end{aligned}
$$

In the previous inequality, we use the fact that F^- is convex and $F^-(\langle u, \boldsymbol{A}u\rangle) \leq \langle u, F^-(\boldsymbol{A})\, u\rangle$ for each unitary vector u. The equality between the first and the last term

implies that $F^{-}\left(\langle e_i, \boldsymbol{A}e_i\rangle\right) = \langle e_i, F^{-}\left(\boldsymbol{A}\right)e_i\rangle$ and $F^{-}\left(\langle e_i, \boldsymbol{B}e_i\rangle\right) = \langle e_i, F^{-}\left(\boldsymbol{B}\right)e_i\rangle$ for all i. Let $\lambda_A = (\lambda_A^{(1)}, ..., \lambda_A^{(n)})$ and $\lambda_B = (\lambda_B^{(1)}, ..., \lambda_B^{(n)})$ be the eigenvalues associated with $\boldsymbol{A}$ and $\boldsymbol{B}$, respectively, arranged in nondecreasing order.

First, let us observe that it is sufficient to study three cases:

- case 1: $\lambda_{AB}^{(1)} < 0$ and $\lambda_{AB}^{(n)} > 0$
- case 2: $\lambda_{AB}^{(n)} \leq 0$
- case 3: $\lambda_{AB}^{(1)} \geq 0$

Now, let us consider case 1.

#Claim 1: Let $i \in [\![1, n]\!]$ such that $\left\langle e_i, \frac{\boldsymbol{A}+\boldsymbol{B}}{2}e_i\right\rangle < 0$, then $\exists j \in [\![1, n]\!]$ and $\exists l \in [\![1, n]\!]$ such that: $\left\langle e_i, \frac{\boldsymbol{A}+B}{2}e_i\right\rangle = \langle e_i, \boldsymbol{A}e_i\rangle = \langle e_i, \boldsymbol{B}e_i\rangle = \lambda_A^{(j)} = \lambda_B^{(l)}$

Proof of the claim:

Since $\left\langle e_i, \frac{\boldsymbol{A}+\boldsymbol{B}}{2}e_i\right\rangle < 0$, one may deduce from *Step 1* that $\left\langle e_i, \frac{\boldsymbol{A}+\boldsymbol{B}}{2}e_i\right\rangle = \langle e_i, \boldsymbol{A}e_i\rangle = \langle e_i, \boldsymbol{B}e_i\rangle$.

Moreover, there exists a doubly stochastic matrix $(a_{\alpha\beta})_{1\leq\alpha,\beta\leq n}$ such that $\langle e_\alpha, \boldsymbol{A}e_\alpha\rangle = \sum_{\beta=1}^{n} a_{\alpha\beta}\lambda_A^{(\beta)}$ for each $\alpha \in [\![1, n]\!]$. Given the fact that $F^{-}\left(\langle e_i, \boldsymbol{A}e_i\rangle\right) = F^{-}\left(\sum_{\beta=1}^{n} a_{i\beta}\lambda_A^{(\beta)}\right) = \langle e_i, F^{-}\left(\boldsymbol{A}\right)e_i\rangle = \sum_{\beta=1}^{n} a_{i\beta}F^{-}\left(\lambda_A^{(\beta)}\right)$ and $\sum_{\beta=1}^{n} a_{i\beta} = 1$ (by the definition of a doubly stochastic matrix), this forces, using again *Step 1* , that $\exists j \in [\![1, n]\!]$ such that $\left\langle e_i, \frac{\boldsymbol{A}+\boldsymbol{B}}{2}e_i\right\rangle = \lambda_A^{(j)}$. A similar proof can be applied to the matrix $\boldsymbol{B}$ to deduce that $\exists l \in [\![1, n]\!]$ such that $\left\langle e_i, \frac{\boldsymbol{A}+\boldsymbol{B}}{2}e_i\right\rangle = \lambda_A^{(l)}$. This achieves the proof of the claim.

#Claim 2: Let $j \in [\![1, n]\!]$ such that $\lambda_A^{(j)} < 0$, then $\exists i \in [\![1, n]\!]$ such that $\left\langle e_i, \frac{\boldsymbol{A}+\boldsymbol{B}}{2}e_i\right\rangle = \langle e_i, \boldsymbol{A}e_i\rangle = \langle e_i, \boldsymbol{B}e_i\rangle = \lambda_A^{(j)}$. The same result holds for the matrix $\boldsymbol{B}$.

Proof of the claim:

First, let us observe that for each $j \in [\![1, n]\!]$, $\exists i \in [\![1, n]\!]$ such that $a_{ij} > 0$, where $(a_{\alpha\beta})_{1\leq\alpha,\beta\leq n}$ is again the doubly stochastic matrix used in the proof of the previous claim. Indeed, this result holds when $(a_{\alpha\beta})_{1\leq\alpha,\beta\leq n}$ is a permutation matrix, then it also holds for each doubly stochastic matrix since the set of the permutation matrices are the extreme points of the convex compact set of the the doubly stochastic matrices. Therefore, using the same argument as in the proof of the previous claim, we obtain the desired result.

From the claims 1 and 2, it is seen that the matrices $\frac{\boldsymbol{A}+\boldsymbol{B}}{2}$, $\boldsymbol{A}$ and $\boldsymbol{B}$ share the same strictly negative eignevalues, assumed to be $\left\{\lambda_{AB}^{(1)} = \lambda_A^{(1)} = \lambda_B^{(1)}, ..., \lambda_{AB}^{(p)} = \lambda_A^{(p)} = \lambda_B^{(p)}\right\}$ ($p \leq n$). Moreover, $\{e_1, ..., e_p\}$ are also the eigenvectors of A associated with $\lambda_A^{(1)}, ..., \lambda_A^{(p)}$, respectively. The same result remains true for the matrix $\boldsymbol{B}$. In fact, we have

$\left\langle e_1, (A - \lambda_A^{(1)} I) e_1 \right\rangle = 0$, since $A - \lambda_A^{(1)} \boldsymbol{I} \geq 0$, then $e_1 \in ker(\boldsymbol{A} - \lambda_A^{(1)} \boldsymbol{I})$. Since $vect\{e_2, ..., e_n\} = vect\{e_1\}^{\perp}$, on may conclude that $vect\{e_2, ..., e_n\}$ is an invariant subspace of $\boldsymbol{A}$. Repeating consecutively the same argument, if necessary, on $vect\{e_k, ..., e_n\}$ $(k \leq p)$ we obtain the desired result. Let W^- be the subspace $vect\{e_1, ..., e_p\}$.

Now, assume that $\langle e_{p+1}, \frac{\boldsymbol{A}+\boldsymbol{B}}{2} e_{p+1} \rangle = 0$, then we necessarily have $\langle e_{p+1}, \boldsymbol{A} e_{p+1} \rangle = 0$ and $\langle e_{p+1}, \boldsymbol{B} e_{p+1} \rangle = 0$ using *Step 1.* Moreover, $vect\{e_{p+1}, ..., e_n\}$ is an invariant subspace of $\boldsymbol{A}$ and $\langle u, \boldsymbol{A}u \rangle \geq 0$ for each unitary vector $u \in vect\{e_{p+1}, ..., e_n\}$. We conclude $\boldsymbol{A} e_{p+1} = 0$. By analogy, we have $\boldsymbol{B} e_{p+1} = 0$. Therefore, $ker(\frac{\boldsymbol{A}+\boldsymbol{B}}{2}) \subseteq ker(\boldsymbol{A})$ and $ker(\frac{\boldsymbol{A}+\boldsymbol{B}}{2}) \subseteq ker(\boldsymbol{B})$.

Let us observe that the claims 1 and 2 achieve the proof in case 2. Indeed, the matrices $\boldsymbol{A}$ and $\boldsymbol{B}$ coincide on the subspaces W^- and $ker(\frac{\boldsymbol{A}+\boldsymbol{B}}{2})$. Moreover, the equality $\mathbb{R}^n = W^- \oplus ker(\frac{\boldsymbol{A}+\boldsymbol{B}}{2})$ implies $\boldsymbol{A} = \boldsymbol{B}$.

Let $\{f_1, ..., f_n\}$ be an orthonormal basis consisting on eigenvectors of $\frac{\boldsymbol{K}(\boldsymbol{A}+\boldsymbol{B})\boldsymbol{K}}{2}$ and $\gamma_{AB} = (\gamma_{AB}^{(1)}, ..., \gamma_{AB}^{(n)})$ are the associated eigenvalues arranged in nondecreasing order. Following similar arguments as before and using the convexity feature of the function F^+, one may conclude that the matrices $\frac{\boldsymbol{K}(\boldsymbol{A}+\boldsymbol{B})\boldsymbol{K}}{2}$, $\boldsymbol{KAK}$ and $\boldsymbol{KBK}$ share the same strictly positive eigenvalues chosen to be $(\gamma_{AB}^{(n-p'+1)}, ..., \gamma_{AB}^{(n)})$ $(p' \geq 1)$ and the associated eigenvectors are $\{f_{n-p'+1}, ..., f_n\}$. In particular, by analogy with the case 2, it is easy to conclude the proof in case 3 using the non singularity of $\boldsymbol{K}$. Let W^+ be the subspace $vect\{f_1, ..., f_p\}$.

Before going further, let us observe that we have proved that the matrices $\boldsymbol{A}$ and $\boldsymbol{B}$ coincide on the following spaces W^-, $ker(\frac{\boldsymbol{A}+\boldsymbol{B}}{2})$ and $\boldsymbol{K}W^+$. To conclude the proof, it is sufficient to establish that $\mathbb{R}^n = W^- \oplus ker(\frac{\boldsymbol{A}+\boldsymbol{B}}{2}) \oplus \boldsymbol{K}W^+$.

#Claim 3: $\boldsymbol{dim}(\boldsymbol{K}W^+) = \boldsymbol{dim}(W^+) = \boldsymbol{dim}(\mathbb{R}^n) - \boldsymbol{dim}(W^-) - \boldsymbol{dim}(ker(\frac{\boldsymbol{A}+B}{2}))$

Proof of the claim:

The minmax principle together with the non singularity of $\boldsymbol{K}$ ensure that:

$$\gamma_{AB}^{(k)} = \max_{\substack{M \subset \mathbb{R}^n \\ dim(M) = n-k+1}} \min_{\substack{x \in M \\ x \neq 0}} \frac{\left\langle x, \frac{\boldsymbol{K}(\boldsymbol{A}+B)\boldsymbol{K}}{2} x \right\rangle}{\|x\|^2} \tag{57a}$$

$$= \max_{\substack{M \subset \mathbb{R}^n \\ dim(M) = n-k+1}} \min_{\substack{x \in M \\ x \neq 0}} \frac{\left\langle x, \frac{(\boldsymbol{A}+B)}{2} x \right\rangle}{\|Kx\|^2} \tag{57b}$$

From the equation (57b) and the non singularity of $\boldsymbol{K}$, one may notice that $\boldsymbol{card}\{k \in [\![1, n]\!] / \gamma_{AB}^{(k)} < 0\} = \boldsymbol{card}\{k \in [\![1, n]\!] / \lambda_{AB}^{(k)} < 0\}$. Moreover, using again

the non singularity of $\boldsymbol{K}$, we have $\boldsymbol{dim}(ker(\frac{\boldsymbol{K}(\boldsymbol{A}+\boldsymbol{B})\boldsymbol{K}}{2})) = \boldsymbol{dim}(ker(\frac{\boldsymbol{A}+\boldsymbol{B}}{2}))$. Therefore, $\boldsymbol{card}\{k \in [\![1,n]\!] / \gamma_{AB}^{(k)} > 0\} = \boldsymbol{card}\{k \in [\![1,n]\!] / \lambda_{AB}^{(k)} > 0\}$. In particular, we have $\boldsymbol{dim}(\boldsymbol{K}W^+) = \boldsymbol{dim}(W^+) = \boldsymbol{dim}(\mathbb{R}^n) - \boldsymbol{dim}(W^-) - \boldsymbol{dim}(ker(\frac{\boldsymbol{A}+\boldsymbol{B}}{2}))$

#Claim 4: $\mathbb{R}^n = W^- \oplus ker(\frac{\boldsymbol{A}+\boldsymbol{B}}{2}) \oplus \boldsymbol{K}W^+$

Proof of the claim:

Indeed, let $(u_1, u_2, u_3) \in W^- \times ker(\frac{\boldsymbol{A}+\boldsymbol{B}}{2}) \times W^+$ such that $u_1+u_2+\boldsymbol{K}u_3 = 0$. We have, $\big\langle (u_1+u_2), \frac{\boldsymbol{A}+\boldsymbol{B}}{2}(u_1+u_2) \big\rangle \leq 0$ and $\big\langle (\boldsymbol{K}u_3), \frac{\boldsymbol{A}+\boldsymbol{B}}{2}(\boldsymbol{K}u_3) \big\rangle \geq 0$. Since $\boldsymbol{K}u_3 = -u_1 - u_2$, one may deduce that $\big\langle (\boldsymbol{K}u_3), \frac{\boldsymbol{A}+\boldsymbol{B}}{2}(\boldsymbol{K}u_3) \big\rangle = 0$ and $\big\langle (u_1+u_2), \frac{\boldsymbol{A}+\boldsymbol{B}}{2}(u_1+u_2) \big\rangle = 0$. Given the invariant feature and the definition of the space W^+, we necessary have $u_3 = 0$. Moreover, we have $u_1+u_2 \in ker(\frac{\boldsymbol{A}+\boldsymbol{B}}{2})$ which implies that $u_1 = 0$ since $W^- \cap ker(\frac{\boldsymbol{A}+\boldsymbol{B}}{2}) = \{0\}$. As a consequence, we have $u_2 = 0$.

Using claim 3, we have $\boldsymbol{dim}(\mathbb{R}^n) = \boldsymbol{dim}(W^-) + \boldsymbol{dim}(ker(\frac{\boldsymbol{A}+\boldsymbol{B}}{2})) + \boldsymbol{dim}(\boldsymbol{K}W^+)$. This achieves the proof of the claim and the proof of the proposition 3.5.

□

References

[1] J. Mazars and G. Pijaudier-Cabot. From damage to fracture mechanics and conversely: A combined approach. *International Journal of Solids and Structures*, 33:3327–3342, 1996.

[2] C.L. La borderie. *Phénoménes unilatéraux dans un matériaux endommageable: modélisation et application à l'analyse des structures en béton.* PhD thesis, Université Paris VI, 1991.

[3] B. Richard, F. Ragueneau, C. Cremona, and L. Adelaide. Isotropic continuum damage mechanics for concrete under cyclic loading: stiffness recovery, inelastic strains and frictional sliding. *Engineering Fracture Mechanics*, 77:1203–1223, 2010.

[4] B. Richard and F. Ragueneau. Continuum damage mechanics based model for quasi-brittle materials subjected to cyclic lloading: Formulation, numerical implementation and applications. *Engineering Fracture Mechanics*, 98:383–406, 2013.

[5] M. Vassaux, B. Richard, F. Ragueneau, A. Millard, and A. Delaplace. Regularised crack behaviour effects on continuum modelling of quasi-brittle materials under cyclic loading. *Engineering Fracture Mechanics*, 149:18–36, 2015.

[6] A. D. Jefferson and I.C. Mihai. The simulation of crack opening closing and aggregate interlock behaviour in finite element concrete models. *International Journal for Numerical Methods in Engineering*, 104:48–78, 2015.

[7] J. OLIVER. MODELLING STRONG DISCONTINUITIES IN SOLID MECHANICS VIA STRAIN SOFTENING CONSTITUTIVE EQUATIONS. PART 1: FUNDAMENTALS. *International Journal for Numerical Methods in Engineering*, 39(21):3575–3600, November 1996.

[8] R. Desmorat. Anisotropic damage modeling of concrete materials. *International Journal of Damage Mechanics*, 25:818–852, 2015.

[9] J.L. Chaboche. Anisotropic creep damage in the framework of continuum damage mechanics. *Nuclear Engineering and Design*, 79:309–319, 1984.

[10] J.L. Chaboche. Damage induced anisotropy: On the difficulties associated with the active/passive unilateral effect. *International Journal of Damage Mechanics*, 1:148–171, 1992.

[11] J. Chaboche and J. Maire. New progress in micromechanics-based cdm models and their application to CMCs. *Composites Science and Technology*, 61:2239–2246, 2000.

[12] F. Leckie and E. Onat. Tensorial nature of damage measuring internal variables. In J. Hult and J. Lemaire, editors, *Physical Non-linearities in Structural Analysis.*, pages 140–155. Springer, Berlin, Heidelberg, 1981.

[13] L. Dormieux and D. Kondo. *Micromechanics of Fracture and Damage.* Wiley, 2016.

[14] J. Cordebois and F. Sidoroff. Anisotropic damage in elasticity and plasticity. *Journal de Mécanique Théorique et Appliqué*, pages 45–60, 1982.

[15] S. Murakami. Mechanical modeling of material damage. *Journal of Applied Mechanics*, 55:280–286, 1988.

[16] P. Ladevèse. On an anisotropic damage theory. In Boehler JP, editor, *Proceedings of the CNRS International College on Failure Criteria of Structured Media*, volume 351, pages 355–363, France: Villars de Lens, 1983.

[17] J. Lemaitre, R. Desmorat, and M. Sauzay. Anisotropic damage law of evolution. *European Journal of Mechanics - A/Solids*, 19:187–208, 2000.

[18] R. Bargellini, D. Halm, and A. Dragon. Modelling of quasi-brittle behaviour: a discrete approach coupling anisotropic damage growth and frictional sliding. *European Journal of Mechanics - A/Solids*, 27:564–581, 2008.

[19] D. Halm and A. Dragon. An anisotropic model of damage and frictional sliding for brittle materials. *European Journal of Mechanics - A/Solids*, 17:439–460, 1998.

[20] Pierre Badel, Vincent Godard, and Jean-Baptiste Leblond. Application of some anisotropic damage model to the prediction of the failure of some complex industrial concrete structure. *International Journal of Solids and Structures*, 44(18-19):5848–5874, September 2007.

[21] P. I. Kattan and G. Z. Voyiadjis. A coupled theory of damage mechanics and finite strain elasto-plasticity i. damage and elastic deformations. *International Journal of Engineering Science*, 28:421–435, 1990.

[22] M. Brunig. An anisotropic ductile damage model based on irreversible thermodynamics. *International Journal of Plasticity*, 19:1679–1713, 2003.

[23] F Cormery and H Welemane. A critical review of some damage models with unilateral effect. *Mechanics Research Communications*, 29(5):391–395, September 2002.

[24] J.L. Chaboche. Development of continuum damage mechanics for elastic solids sustaining anisotropic abd unilateral damage. *International Journal of Damage Mechanics*, 2:311–329, 1993.

[25] J.C. Simo and J.W. Ju. Strain- and stress-based continuum damage models-i. Formulation. *International Journal of Solids and Structures*, 23:821–840, 1987.

[26] M. Ortiz. A constitutive theory for the inelastic behavior of concrete. *Mechanics of Materials*, 4:67–93, 1985.

[27] Ignacio Carol, Egidio Rizzi, and Kaspar Willam. On the formulation of anisotropic elastic degradation. i. theory based on a pseudo-logarithmic damage tensor rate. *International Journal of Solids and Structures*, 38(4):491–518, January 2001.

[28] I. Carol, E. Rizzic, and K. Willam. On the formulation of anisotropic elastic degradation.: Ii. generalized pseudo-rankine model for tensile damage. *International Journal of Solids and Structures*, 2001.

[29] N. Challamel, C. Lanos, and C. Casandjian. Strain-based anisotropic damage modelling and unilateral effects. *International Journal of Mechanical Sciences*, 47:459–473, 2005.

[30] A. Alliche and H. Dumontet. Anisotropic model of damage for geomaterials and concrete. *International Journal for Numerical and Analytical Methods in Geomechanics*, 35:969–979, 2011.

[31] A. Menzel and P. Steinmann. A theoretical and computational framework for anisotropic continuum damage mechanics at large strains. *International Journal of Solids and Structures*, 38:9505–9523, 2001.

[32] E.A. Carlen. Trace inequalities and quantum entropy. an introductory course. *Contemporary Mathematics*, 529:73–140, 2010.

[33] A. Sellier, G. Casaux-Ginestet, L. Buffo-Lacarrière, and X. Bourbon. Orthotropic damage coupled with localized crack reclosure processing. part i: Constitutive laws. *Engineering Fracture Mechanics*, 97:148–167, jan 2013.

[34] J.B. Hiriart-Urruty and C. Lemaréchal. *Fundamentals of Convex Analysis*, volume 305 and 306 of *Grundlehren Text Editions*. Springer-Verlag Berlin Heidelberg, 2001.

[35] J. Lemaitre and R. Desmorat. *Engineering Damage Mechanic: Ductile, Creep, Fatigue and Britlle failure*. Berlin: Springer, 2005.

[36] H.W. Reinhardt and H.A.W. Cornelissen. Post-peak cyclic behaviour of concrete in uniaxial tensile and alternating tensile and compressive loading. *Cement and Concrete Research*, 14:263–270, 1984.

[37] R. Bhatia. *Matrix Analysis*, volume 169 of *Graduate Texts in Mathematics*. Springer New York, 1997.

[38] F. Hiai and D. Petz. *Introduction to Matrix Analysis and Applications*. Universitext. Springer International Publishing, 2014.

[39] H. Brezis. *Functional Analysis, Sobolev Spaces and Partial Differential Equations*. Universitext. Springer-Verlag New York, 2011.

[40] P. Krejci. *Hysteresis, convexity and dissipation in hyperbolic equations*. Gakkotosho,Tokyo, 1996.

[41] R. Desmorat, F. Gatuingt, and F. Ragueneau. Nonlocal anisotropic damage model and related computational aspects for quasi-brittle materials. *Engineering Fracture Mechanics*, 74:1539–1560, 2007.

[42] J. Mazars. *Application de la mécanique de léndommagement au comportement non linèaire et à la rupture du béton de structure*. PhD thesis, Université Paris 6, 1984.

[43] Gilles Pijaudier-Cabot and Zdeněk P. Bažant. Nonlocal damage theory. *Journal of Engineering Mechanics*, 113(10):1512–1533, October 1987.

[44] C. Giry, F. Dufour, and J. Mazars. Stress-based nonlocal damage model. *International Journal of Solids and Structures*, 48:3431–3443, 2011.

[45] M. Jirasek. Nonlocal models for damage and fracture: Comparison of approachs. *International Journal of Solids and Structures*, 35:4133–4145, 1998.

[46] Z. Bazant and G. Pijaudier-Cabot. Measurement of characteristic length of nonlocal continuum,. *Journal of Engineering Mechanics*, 115:755–767, 1989.

[47] H. Egner, J. J. Skrzypek, and W. Egner. Effect of characteristic length on nonlocal prediction of damage and fracture in concrete. *Journal of Theoretical and Applied Mechanics*, 44:485–503, 2006.

[48] C. Comi and U. Perego. Criteria for mesh refinement in nonlocal damage finite element analyses. *European Journal of Mechanics - A/Solids*, 23:615–632, 2004.

[49] J. Alfaiate, G.N. Wells, and L.J. Sluys. Strong embedded discontinuities for simulating fracture in quasi-brittle materials. In *de Borst, R., Mazars, J., Pijaudier-Cabot, G., and Van Mier, J.G.M., editors, Fourth International Conference on Fracture Mechanics of Concrete and Concrete Structure*, pages 749–756, 2001.

[50] C. Shi, A.G. van Dam, J.G.M. van Mier, and B. Sluys. Crack interaction in concrete. In F. H. Wittmann, editor, *Materials for Buildings and Structures*, pages 125–131. Wiley-VCH Verlag, 2005.

List of Figures

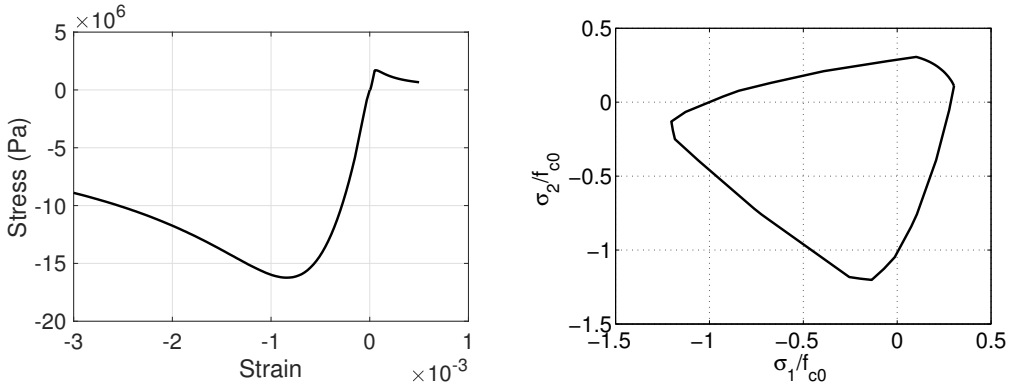

(a) Uniaxial response.

(b) Failure surface.

Figure 1: Local responses in uni-axial and bi-axial loading.

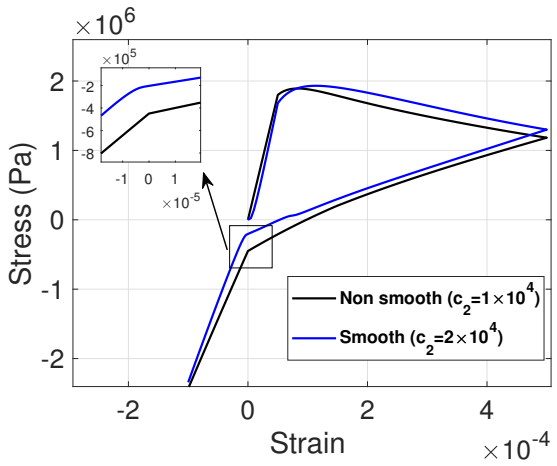

Figure 2: Effect of the regularity of the opening (closure) cracking functions on the uniaxial response.

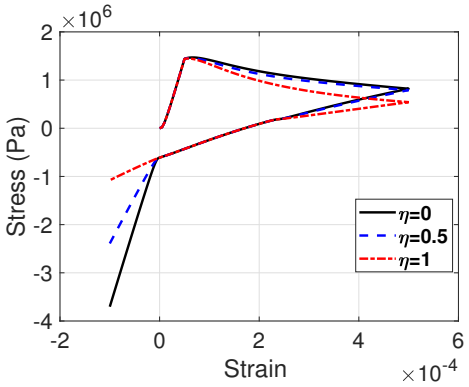

(a) η effect.

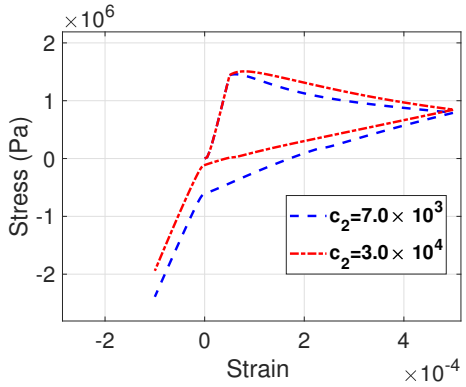

(b) c_2 effect.

Figure 3: Effect of the parameter η and the constant c_2 on the uniaxial response.

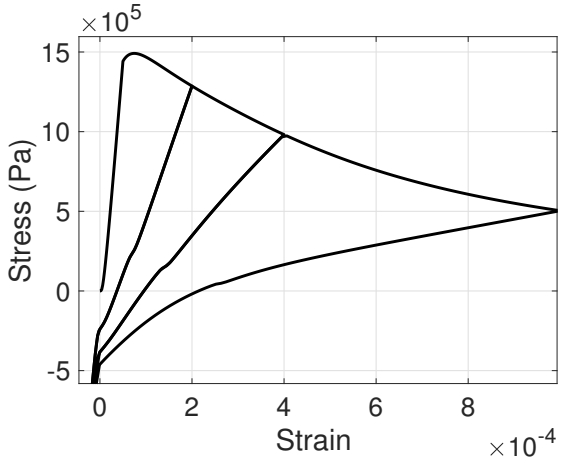

Figure 4: Cyclic response of the model using $\eta = 1$, $c_2 = 10^4$ and $c_1 = 10^{-5}$.

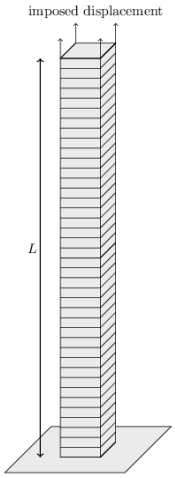

(a)

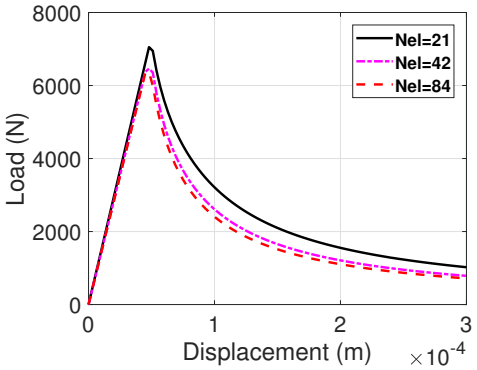

(b)

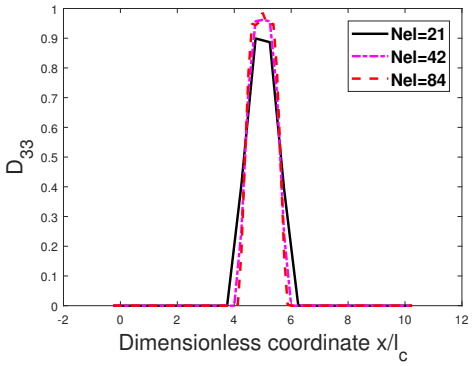

(c)

Figure 5: The finite element mesh for the three-dimensional bar (a). The uniaxial responses (b) and the damage profiles (c) for different meshes: Nel=21,42 and 84.

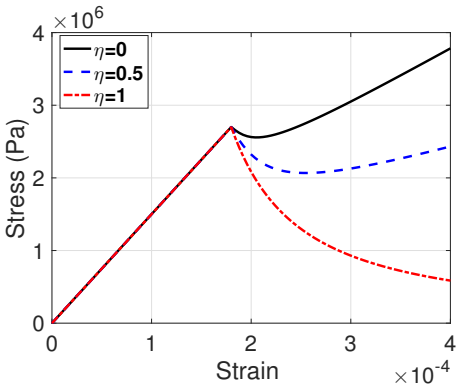

Figure 6: Effect of the parameter η on the shear response.

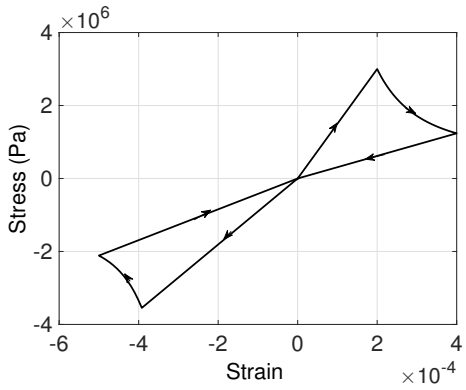

Figure 7: Shear response for cyclic loading path -proposed model.

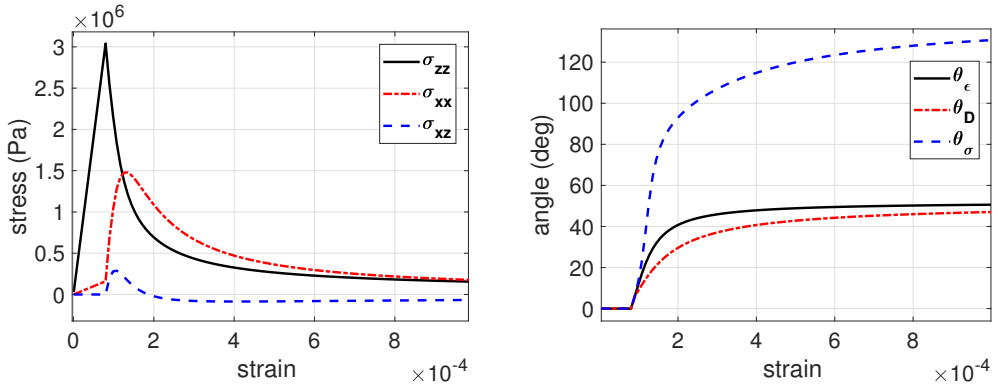

(a) Strain-stress curves.

(b) Strain-angle curves.

Figure 8: Stress and angle evolutions for Willam's test using the proposed model.

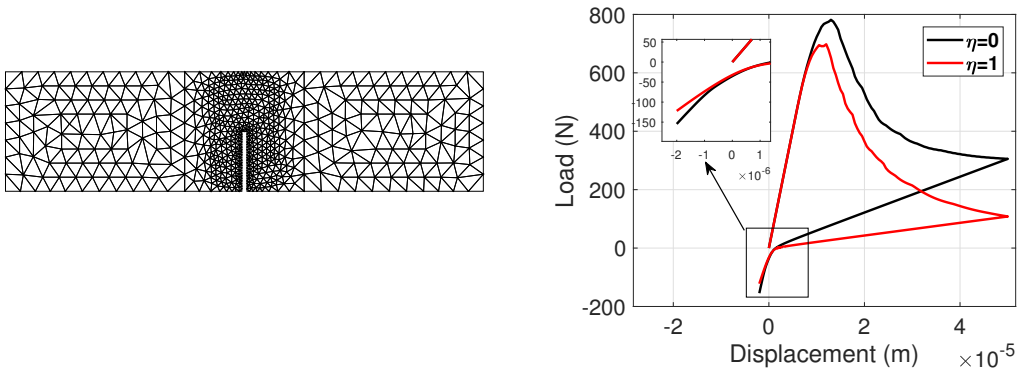

(a) Mesh with 1186 elements.

(b) Load-displacement curve.

Figure 9: Finite element mesh and reaction curve (three point bending test).

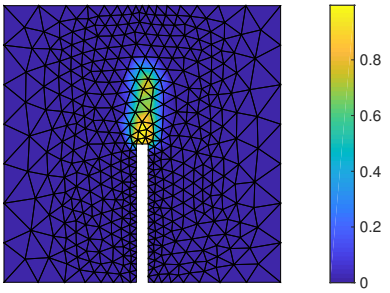

(a) D_{11}.

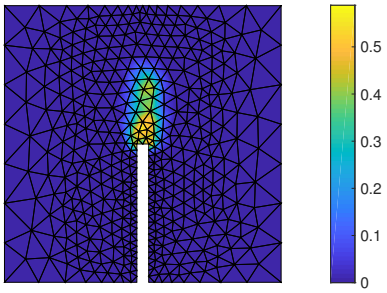

(b) D_{22}.

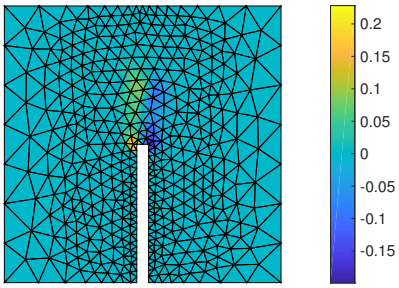

(c) D_{12}.

Figure 10: Damage isovalues for each component for $\eta = 0$.

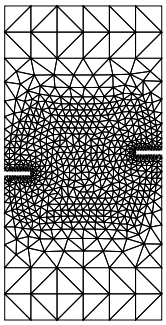

(a) Mesh with 1228 triangular elements.

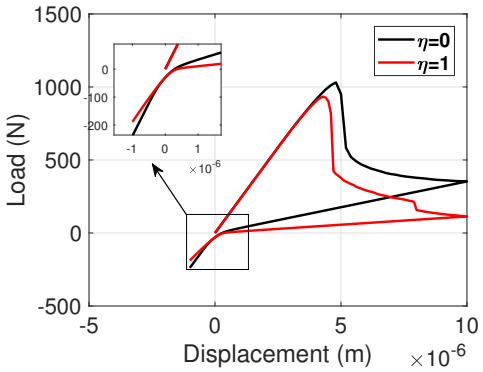

(b) Load-displacement curve.

Figure 11: Finite element mesh and reaction curve (Shi's test).

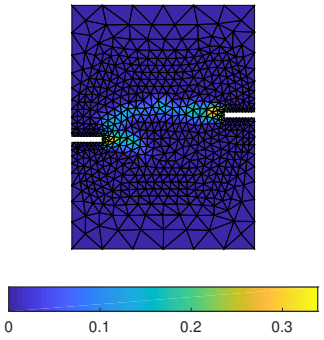

(a) D_{11}.

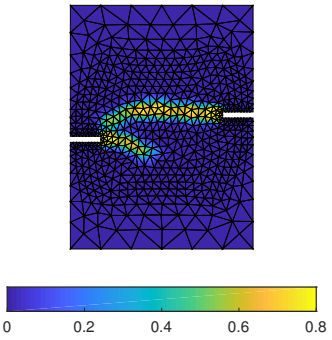

(b) D_{22}.

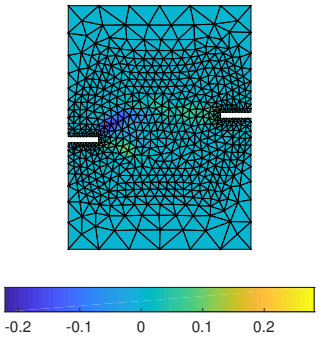

(c) D_{12}.

Figure 12: Damage isovalues for each component in the neighborhood of the notches for $\eta = 0$.